Energy Conversion and Management 348 (2026) 120711

Contents lists available at ScienceDirect

Energy Conversion and Management

journal homepage: www.elsevier.com/locate/enconman

Research paper

Potential geothermal deployments for U.S. electricity and industrial heat

Chen Chen, Daniel S. Cohan *

Department of Civil and Environmental Engineering, Rice University, 6100 Main St., Houston, 77005, TX, United States

ARTICLE INFO

Keywords:
Geothermal
EGS
Direct-use heating
Decarbonization
Sector-coupled model
Energy system modeling

ABSTRACT

Geothermal energy can be used for power generation and for the direct use of heat in buildings and industrial and agricultural applications. Recent advancements, including improvements in drilling technologies, have reduced the anticipated costs of enhanced geothermal systems (EGS), which are engineered reservoirs that extract heat from hot, dry rock by creating permeability through hydraulic stimulation. Advances in EGS for electricity production could also be expected to expand opportunities for deep direct-use (DDU) geothermal systems, which provide low- and medium-temperature heat for industrial process heating (IPH).

This study analyzes geothermal deployment potential in the United States, focusing on EGS for power generation and DDU for IPH. We employ a sector-coupled energy system model to evaluate the technical and economic feasibility of geothermal integration accounting for industry-specific temperature needs, resource availability, and policy constraints, considering uncertainties from fuel prices and alternative cost assumptions. The model computes the mix of resources that minimizes overall system costs. The cost-minimizing system features nearly 40 GW_e of EGS electrical capacity, mostly in Western states, and 30 GW_{th} of thermal DDU deployment, mainly to replace industrial heat at temperatures ranging from 100 to 200 °C. Finally, we compute the CO_2 emission reductions that can be achieved by the IPH applications.

1. Introduction

Geothermal energy can provide a low-carbon resource for power generation, heating and cooling applications, and energy storage, and other purposes due to its scalability, round-the-clock availability, and minimal land footprint. Learning-by-doing could enhance the cost-effectiveness of geothermal energy as drilling technologies continue to improve. Historically, geothermal power plants and direct-use systems in the United States have utilized hydrothermal reservoirs at depths of less than 2 km [1,2]. These high-quality resources are mainly concentrated in western states such as California and Nevada, where nearly all of today's 4 GW of geothermal electricity capacity (GW_e) and around 100 direct-use systems, with 400 MW of thermal capacity (MW_{th}), are located [3–5].

Deployment beyond hydrothermal regions will require unconventional technologies such as enhanced geothermal systems (EGS) for power generation or direct use heating. EGS improves the permeability of geothermal systems through hydraulic, chemical, and thermal stimulation in regions where fluid volumes and rock permeability are not sufficient to permit economic extraction using traditional techniques [6]. The stimulated system then injects water or supercritical CO_2 into hot dry rock, with the heated liquid or steam brought to the surface via an open-loop for direct use or to turn a turbine to generate electricity [7]. Direct use heating can provide heat to dry crops, pasteurize dairy products, or serve other industrial purposes.

Previous studies have examined opportunities for geothermal power generation [8–12]. Typical geothermal heating systems use a two-well layout — one for production and one for reinjection — and are designed for efficient, long-term operation (30+ years) [13,14], though variations exist depending on site conditions and project design [15,16]. Long-lasting examples include a low-enthalpy system in Iceland that has operated since the 1930s [17]. Studies have demonstrated the value of geothermal for low-temperature heating applications below 150 °C [2,4,18,19].

Many studies have focused options for reducing CO_2 emissions in the electricity sector both globally [20–23] and in the United States [24–28]. Geothermal energy provides a low-carbon dispatchable option to complement variable renewable energy (VRE) resources such as wind and solar.

In the U.S., industrial energy use accounts for nearly one-third of all primary energy consumption [29]. The 2018 Manufacturing Energy Consumption Survey (MECS) reports 20.7 exajoules (EJ) (5750 TWh) of thermal and electrical energy consumption [30]. Industrial process heat

* Corresponding author.
E-mail addresses: cc143@rice.edu (C. Chen), cohan@rice.edu (D.S. Cohan).
URLs: https://chenchen.page/ (C. Chen), https://cohan.rice.edu/ (D.S. Cohan).

https://doi.org/10.1016/j.enconman.2025.120711
Received 8 July 2025; Received in revised form 26 September 2025; Accepted 24 October 2025
Available online 4 November 2025

(IPH) involves the use of thermal energy for manufacturing purposes, accounting for about 9% of all U.S. CO_2 emissions [31]. In 2018, energy use for IPH was nearly 3250 TWh, accounting for approximately 56.5% of total manufacturing energy consumption [30]. In 2022, the U.S. Department of Energy (DOE) launched the Industrial Heat Shot aiming to develop cost-competitive decarbonization technologies that can reduce industrial heat greenhouse gas emissions by at least 85% by 2035 [32].

Low and medium-temperature IPH (below 200 °C) represents approximately 35% of total thermal energy use of IPH and contributes around 3.5% of the U.S.'s energy-related greenhouse gas emissions [33]. Due to its significance as an emissions source, low-temperature IPH is now a target for alternative, lower-carbon technologies such as geothermal, solar thermal, biomass, heat pumps, and waste heat (e.g., [34–39]). Currently only 20% of this heat is supplied by biofuel or waste fuels, which are used mainly in the pulp and paper industry [40]. Among the alternatives, geothermal energy for IPH in the U.S. has high potential yet has been relatively underexplored. While only 1.1 TWh of geothermal energy was used for IPH in 2023 [41], the U.S. DOE GeoVision study indicates a potential geothermal resource of over 7,800,000 TWh of thermal energy within U.S. sedimentary basins [11].

Geothermal energy has seen rapid advancements recently, driven by increasing demand for reliable, dispatchable renewable power. Fervo Energy's Project Cape in Milford Valley, Utah, successfully drilled four horizontal wells, achieving depths of 8150 to 8550 ft (or 2500 to 2600 m) with lateral sections extending 5000 ft (or 1500 m). The project demonstrated a 70% reduction in drilling times, with costs dropping from $9.4 million to $4.8 million per well within just six months [42]. Additionally, Sage Geosystems secured a 150 MW power purchase agreement to supply Meta data centers with geothermal energy [43]. The company is also developing a 3 MW geo-pressured system in Texas, capable of providing up to 18 h of long-term energy storage [44]. Since 2017, the U.S. Department of Energy (DOE) Geothermal Technologies Office funded six deep direct-use (DDU) projects by aims to catalyze broader adoption of DDU systems by enhancing the understanding of their technical performance and economic viability, thereby paving the way for broader implementation [19,45–49].

Decarbonizing IPH can be achieved via low-carbon fuels or electrification [50,51]. Previous studies have shown that power-to-heat technologies could be a cost-effective strategy for decarbonizing a large portion of the heat sector [33,52–54]. To accurately assess the economic competitiveness of geothermal DDU systems against electrification, a sector-coupled energy model is necessary. Such a model evaluates both decarbonization pathways simultaneously, offering a more holistic view than separate models for power and heating [54–56].

Sector-coupled energy models have been used to identify decarbonization strategies across sectors including electricity, industrial, residential, commercial, and transportation. Most existing models focus only on electricity, overlooking network dynamics, resource limits, and cross-sector interdependencies. Integrated models have proven effective in identifying multi-sector strategies [57–61], though most focus on Europe with limited U.S. applications [62,63]. While previous studies have explored alternative renewable and electrified solutions for decarbonizing industrial heat, none have yet examined a cost-optimized, future-oriented system using a sector-coupled capacity expansion model that integrates the power and heating sectors in the United States. Multi-sector integrated modeling can help inform comprehensive decarbonization strategies.

This study aims to assess the potential of geothermal energy for both power generation and IPH, using a sector-coupled energy model that integrates the power and industrial sectors—the two most energy-intensive domains in the United States. The analysis incorporates the latest cost estimates and resource assessments for EGS and DDU systems, reflecting significant cost reductions compared to previous studies.

The model analyzes trade-offs between generating electricity and meeting IPH demands, with detailed breakdowns by North American Industrial Classification System (NAICS) codes and specific temperature requirements. With high temporal and spatial resolution, the model addresses transmission network bottlenecks within interconnections, pinpoints locations for geothermal IPH demand and resource availability, and effectively captures the variability of renewable energy resources.

To our knowledge, this paper is the first to jointly assess opportunities for geothermal energy to provide electricity and industrial heat at the individual facility level in the United States. In addition, our use of a sector-coupled framework rather than a single-sector model highlights the interdependencies between the power and industrial sectors. The overall modeling workflow and key steps are summarized in Table 1.

2. Methods

We employed a sector-coupled energy system model to determine the cost-optimized configuration for meeting both power and heating demands in the continental United States (Fig. 1). Fossil fuel resources such as coal, natural gas, and oil were modeled as dual-purpose, capable of generating electricity or supplying direct heat for industrial processes. Similarly, geothermal resources were represented with dual functionality: Enhanced Geothermal Systems (EGS) for electricity generation or Deep Direct-Use (DDU) geothermal systems for industrial process heating (IPH). Nuclear, solar, and wind resources were restricted to electricity generation within the modeling framework, while battery systems were included to store excess power. Resources for thermal energy storage were not considered. Power-to-heat technologies, including resistance heaters and industrial heat pumps, were included as options for IPH.

Although other geothermal technologies are also under development, such as Advanced Geothermal Systems (AGS; [15]) and single-well designs [16], this study focuses only on EGS, defined by the creation of man-made reservoirs in hot dry rocks through drilling and water injection to induce permeability [64]. EGS is an open-loop system where heat is exchanged in fracture networks, in contrast to the closed-loop designs of AGS and single-well systems [65].

We assumed that DDU heat employs the same drilling practices as EGS electricity generation but differs in surface plant configuration [66,67]. Both technologies can drill to depths of up to 7 km with reservoir temperatures of 150–300 °C, leveraging updated drilling curves reflecting recent advancements that significantly reduce costs and time [68]. We assumed that EGS power generation uses binary cycle power plants with organic Rankine cycles (ORC), with capital costs of $3000 per kW [69,70]. DDU, on the other hand, adopts district heating configurations where geothermal heat is transferred directly to end-users through heat exchangers, with heat exchangers to transfer geothermal heat, costing $100 per kW [2,67,71].

2.1. Sector-coupled power and heating model

2.1.1. Base model

Python for Power System Analysis for the United States of America (PyPSA-USA; [72]) is an open-source model building upon the electricity system modeling framework PyPSA [73]. It solves a multi-period optimal power flow problem by optimizing linearized load flow equations and the capacity expansion of generators, energy storage units, and the transmission network infrastructure.

The objective function of the cost minimization problem contains all the costs associated with the modeled technologies and infrastructure used to satisfy both electricity and heat demands and additional constraints. The decision variables of the linear problem are the installed capacities and their hourly dispatch. Incurred costs include fixed costs for the capacity expansion (new capacity) and variable costs for hourly operation (all capacity). Fixed costs comprise discounted annualized

Table 1
Overview of the modeling workflow in this study.

Step	Component	Description
1	Electricity System Inputs	Gather and update U.S. data on generation capacity, demand, weather patterns, fuel and capital costs, O&M costs, and relevant policies.
2	Industrial Heating Inputs	Compile facility locations, heat demand profiles, and fuel cost data for industrial process heating across the conterminous U.S.
3	Geothermal Techno-Economic Assessment	Estimate county-level techno-economic performance of EGS and DDU systems using temperature-at-depth profiles and cost parameters.
4	Sector-Coupled Energy Modeling	Optimize generation, transmission, and industrial process heating supply to minimize total system costs across sectors.
5	Sensitivity Analysis	Evaluate the impacts of fuel price changes and policy shifts, including Inflation Reduction Act repeal, on geothermal and other energy deployments.

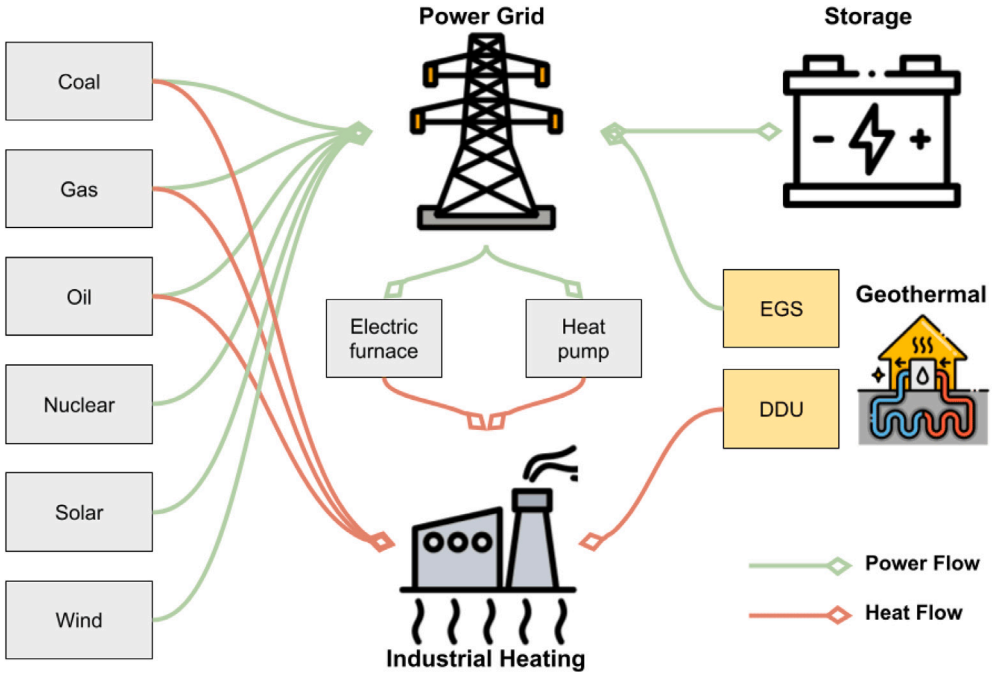

Fig. 1. Schematic chart of power/heating sector-coupled modeling.

investments (new capacity) as well as fixed operation and maintenance (FOM) costs (all capacity). Retirement of existing plants occurs when demands could be met by more cost-effective technology options on a systemwide basis. Variable costs include both fuel expenses and variable O&M (VOM) costs. Eq. (1) presents the simplified objective function of the model, while the complete formulation is provided in Appendix A.

$$\min \text{ System Cost} = \underbrace{\text{Capital Costs}}_{\text{new capacity}} + \underbrace{\text{Fixed O\&M}}_{\text{existing + new}} + \underbrace{\text{Variable O\&M + Fuel}}_{\text{operations over time}} \quad (1)$$

s.t. (1) Generation and heating outputs are within capacity limits,
(2) Storage charging/discharging and state-of-charge balance are maintained,
(3) Transmission flows remain within branch limits,
(4) Power balance: generation + storage supply = electricity demand,
(5) Heat balance: heating supply = industrial heat demand,
(6) Planning reserve margin (PRM) requirements are met,

PyPSA-USA leverages Atlite to provide hourly weather data for the year 2019, spatially resolved on a 30 km × 30 km grid [74]. The data was used to estimate the wind and solar generation availability per snapshot and region (described in Section 2.1.2). We also used the temperature data to estimate the geothermal heat exchange efficiency Appendix D and the efficiency of industrial heat pumps [75].

We selected 2030 as the base model year, using projected electricity demand and power generation technology costs for that year. For IPH, due to limited projections for 2030 and the focus on assessing the potential for geothermal DDU or electrification to replace existing fossil fuel-based heating, the study relies on historical demand. Capital costs are taken from projections for 2030, if such projections are available, and from recent literature for other heating technologies (see Section 2.1.3).

2.1.2. *Electricity*

The base network is built from a synthetic nodal network developed by Breakthrough Energy and Texas A&M University with over 82,000 buses and 41,000 substations in the continental U.S. [76]. All buses and substations were clustered into 134 Regional Energy Deployment System (ReEDS) Balancing Authorities [77]. The Interface Transmission Limits (ITLs) between zones are built from the North American Renewable Integration Study (NARIS) non-synthetic nodal network for the

U.S. electricity system [78,79]. The temporal resolution is three hours, representing a compromise between computational tractability on the one hand and considering a large range of operating conditions that are vital to investment planning on the other.

The electricity balance is the main equation to be satisfied in the power sector, where the total electricity generation, demand, transmission flow, and transmission losses need to be in balance at every time step. Forecasted demand for 2030 is exogenously sourced from the medium electrification scenario of the National Renewable Energy Laboratory (NREL) Electrification Futures Study (EFS; [80]).

On the supply side, characteristics of existing facilities are taken from the 2023 Form EIA-860 open database of conventional power plants, recategorized into the following categories: coal, open-cycle gas turbines (OCGT), combined-cycle gas turbines (CCGT), oil, solar, onshore wind, nuclear, hydrothermal, biomass, and hydropower [29]. We assume that existing battery storage projects have 2-h duration with round-trip efficiency of 90%. The database provides heat rate, efficiency, and unit commitment parameters including ramp-up rate, start-up cost, minimum up and down time, summer or winter derate, etc. We neglected unplanned outages. To account for planned installation prior to 2030, we also included EIA 860M Preliminary Monthly Electric Generator Inventory for projects with regulatory approval or already under construction [81]. Although by 2030 some existing facilities, particularly coal and natural gas plants, may exceed their design lifetimes, we retained them in the model without mandatory retirement unless they become economically unviable. This approach optimizes capacities for generation, storage, and transmission infrastructure by building or retiring resources and progressing toward an optimal system layout.

Capacity installations and retirements are determined based on economic favorability, considering upfront capital costs (new capacity only), O&M costs, and fuel costs. New components are parameterized by expected future costs, operational characteristics, technical capacity potential, and resource availability constraints. PyPSA-USA utilizes forecasted costs and lifetime for technologies available in the NREL Annual Technology Baseline (ATB) for 2030 [82]. Besides all plant types that exist today, the model also considered the addition of EGS, small modular reactors (SMR), and a long-duration battery storage system (8-h) as available solutions to generate and store dispatchable power.

The model incorporates a capacity reserve margin for each Independent System Operator (ISO) based on the reserve margin required by individual ISOs [83]. These margins ensure sufficient generation capacity to address unexpected events, such as power plant outages, which are not explicitly accounted for in the model. The planned reserve margins are 13.75% for the Electric Reliability Council of Texas (ERCOT), 17.6% for the Western Electricity Coordinating Council (WECC), 19% for the Southwest Power Pool (SPP), 15% for the SERC Reliability Corporation (SERC), 15% for the Northeast Power Coordinating Council (NPCC), 20.1% for the Midcontinent Independent System Operator (MISO), and 14.7% for PJM Interconnection (PJM). Capacity reserves are essential to maintaining grid reliability under unforeseen circumstances.

2.1.3. Industrial process heat (IPH)

The model balances IPH demands and heat generation in each time step at all sites. We adopted IPH demand data from McMillan and Ruth [40], which was built upon the facility-level combustion greenhouse gas (GHG) emissions reported under the U.S. Environmental Protection Agency (EPA) Greenhouse Gas Reporting Program (GHGRP) and default emissions factors to estimate the energy value of combustion fuels [84]. The dataset contains the heating demand and fuel use per facility from 2010 to 2015, separated by six-digit NAICS codes and the temperature range of the heat provided.

We aggregated the six-year averaged raw data to the county level, focusing only on heating demand from coal, gas, and oil, while excluding biomass-based heating as it is considered carbon-neutral. National IPH demand is 1530 TWh annually. We assumed that IPH demand stays at the averaged levels from 2010–2015 and assessed the potential of electrification (i.e., resistance heating and heat pump) and geothermal DDU to replace heating that had been provided by fossil fuels. Fig. 2 and Table B.1 in Appendix B summarize the annual demand and CO_2 emissions for all NAICS industries included from McMillan and Ruth [84].

Petroleum refineries have the highest heat demand, at more than 600 TWh annually, including 63% at temperatures of 200–300 °C, a range that could be satisfied by geothermal heat. Other industries, such as alkali and chlorine manufacturing, potash, soda, and borate mining, wet corn milling, organic chemical manufacturing, and plastics manufacturing, also have over 75% of their heat demand below 300 °C, indicating strong potential for geothermal DDU integration. For high-temperature industries like iron and steel mills or lime manufacturing, geothermal heat is insufficient, making electrification with industrial electric boilers a more plausible decarbonization solution.

In the model, the annual county-level IPH demand by NAICS codes and temperature was distributed across buses and hours throughout the year. For each bus in a county, we allocated the demand to the bus based on the bus population density data from the network developed by Breakthrough Energy [76]. Temporally, the distribution followed load profiles from the Electric Power Research Institute (EPRI) Load Shape Library Version 8.0 [85], which categorizes IPH demand by region, hour, and peak/off-peak season, allowing hourly demand to be allocated from annual demand. The hourly bus-level IPH demand by NAICS and temperature was then aggregated based on user-defined inputs, such as the ReEDS balancing areas and 3-h intervals used in this study.

For initial heating supply, we assumed the capacity of existing gas, coal, and oil boilers based on annualized demand and fixed capacity factors (Table 2). Additions in heating capacity were selected from the following heating options: steam boilers burning coal, gas, and oil; electrical resistance heaters; industrial heat pumps; and geothermal DDU. The new generators of thermal energy are matched to industry heat demand based solely on temperature and assumed average heat output in megawatts thermal (MW_{th}). Techno-economic assumptions for fossil-fuel boilers, electrical resistance heaters, and industrial heat pumps were sourced from existing studies [33,86–88] and summarized in Table 2. For geothermal DDU systems, we used a separate techno-economic model to estimate performance, detailed in Section 2.2.2.

The overnight capital costs and O&M costs for those technologies except geothermal DDU systems were mainly sourced from IRENA [87] and Rissman [33]. Fuel costs for coal, gas, and oil are adjusted based on temporal and regional variations across states and balancing authorities (Section 2.1.4). For electric heating options, no additional fuel costs are included as the electricity costs were optimized within the power sector. Fossil fuels and electric boilers can deliver a wide range of supply temperatures, while industrial heat pumps are limited to a maximum of 180 °C [33]. Geothermal DDU systems offer a flexible temperature range of 50 to 300 °C, dependent on local resource conditions (Section 2.2.1).

Efficiency assumptions are generally high across technologies compared to power generating, particularly for industrial heat pumps, which achieve 130%–520% efficiency depending on ambient temperature and the temperature needed for the industrial process [33,88]. For geothermal DDU, we adopted a 90% efficiency from production fluid to end-use [67]. Capacity factors (CF) differ among technologies; fossil fuel heating systems and electric boilers were assumed to have a CF of 85% [33], and industrial heat pumps were assumed to have a CF of 50% under mild climate ([92,95]. The CF for geothermal DDU was based on global data collected by International Geothermal Association (IGA; [94]), ranging from 5.8 to 80.8% depending on the country; in this study, we capped CF at 70% for geothermal DDU. Additional sensitivity analysis on the DDU capacity factors was also conducted. The assumed lifetimes for all technologies range between 18 and 30 years [33,67,87].

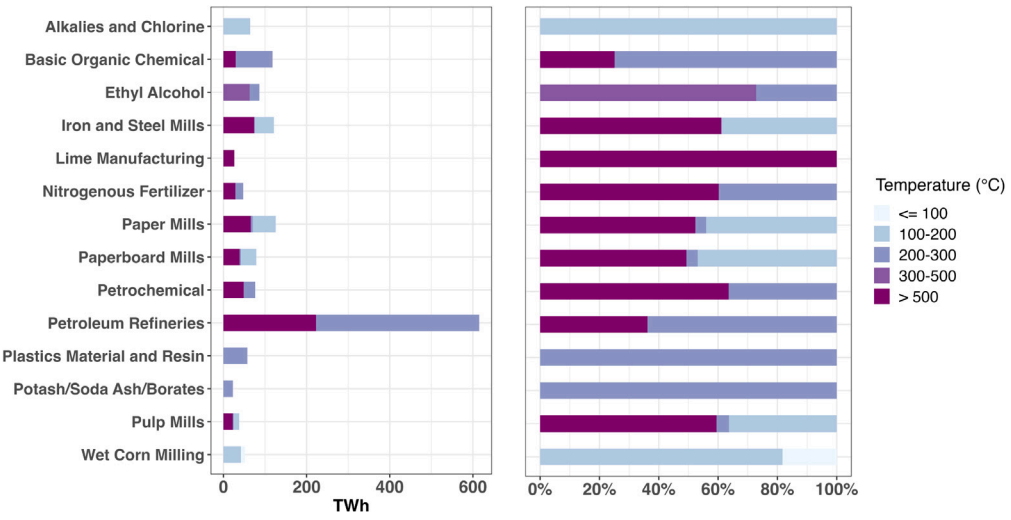

Fig. 2. Annual IPH demand (TWh) (**left**) and percent share (**right**) in each NAICS industry by temperature range (° C).

Table 2
Heating technologies to supply IPH demand in this study (costs under 2024 dollar year).

Fuel	Technology	Overnight cost ($/kW$_{th}$)	O&M cost ($/kW$_{th}$/yr)	Fuel cost ($/MWh)	Temp. range (°C)	Efficiency	Cap. factor	Lifetime	CO_2 emission factor (t/MWh)
Coal	Boiler	471[a]	10[a]	3.1–76.4[b]	Unlimited	81%[c]	85%[a]	25[a]	0.33[d]
Gas	Boiler	132[a]	3[a]	3.1–76.6[b]	Unlimited	75%[c]	85%[a]	25[a]	0.18[d]
Oil	Boiler	263[a]	7[a]	3–295.9[b]	Unlimited	83%[c]	85%[a]	25[a]	0.25[d]
Electricity	Resistance heater	189[e]	8[a]	Reported from Model	Unlimited	99%[c]	85%[e]	18[e]	0
Electricity	Heat pump	938[e]	11[e]	Reported from Model	<180[f]	130–520%[g]	50%[f]	20[g]	0
Geothermal	Direct use	709–3,227[h]	35–138[h]	0	50–300[h]	90%[h]	70%[i]	30[h]	0

[a] IRENA REmap 2030 Technology Cost [87].
[b] EIA 923 fuel prices of 2019 [89].
[c] Schoeneberger et al. [90].
[d] Carbon Dioxide Emissions Coefficients [91].
[e] Rissman [33].
[f] Leak [92].
[g] Jibran S. Zuberi et al. [93].
[h] Beckers & Ross (2023) [67]. The cost variations reflect differences in the depth and temperature gradient of geothermal resources across various locations. This variability affects the feasibility and economic viability of geothermal energy projects, making site-specific analysis crucial.
[i] Geothermal Energy Database [94].

2.1.4. Fuel costs

Fuel costs in the model were extracted from the EIA Application Programming Interface (API) portal, which provides costs for various fuels for both power generation and industrial heating from Form EIA-923 [96]. The dataset is resolved annually or monthly for U.S. states or regions, with prices provided in dollars per thousand cubic feet for natural gas, dollars per short ton for coal, and dollars per gallon for heating oil. All fuel costs were also converted to a 2024 dollar year.

In this study, we extracted the fuel costs of coal, gas, and heating oil in the year 2023 from EIA, and single-point unit-level generator fuel efficiencies from a continuous emissions monitoring systems (CEMS) based dataset [97], to convert all raw fuel prices to dollars per MWh for consistency within the model. For power generators not included in CEMS and all industrial heating applications, a constant efficiency per fuel type is used to convert from $/mmbtu to $/MWh. To address future price uncertainties, the study also includes sensitivity scenarios with varying gas prices.

For coal, EIA provides retail prices for electric utilities but does not include prices specific to industrial heating. According to the EIA annual coal report [98], the average delivered price for industrial coal has historically ranged between 2- and 2.3-times electric power coal prices from 2013 to 2022. In this study, we applied a factor of 2.1 to EIA's raw coal prices to approximate industrial heating fuel costs.

This study does not model evolving fossil fuel reserves explicitly. Future work could incorporate reserve dynamics to capture the effects of technological progress on long-term fuel availability and costs.

2.1.5. Policy constraints

The model estimates the CO_2 emissions from both power and heating sectors based on the emission factors of fossil fuel plants and heat-generating equipment. In this study, we focused on two scenarios of CO_2 emission limits.

The BAU scenario considers existing state, regional, and federal policies as of October 2024. California's Global Warming Solution Act of 2006 (Assembly Bill 398) established a program to reduce economy-wide greenhouse gas emissions to 1990 levels by 40% in California [99]. In Oregon, House Bill (HB) 2021 requires a 20% emissions cuts for electricity providers by 2030 [100] For the Eastern Interconnection, the Regional Greenhouse Gas Initiative (RGGI) cap-and-trade program limits the CO_2 emissions for fossil fuel-fired power plants in eleven states: Connecticut, Delaware, Maine, Maryland, Massachusetts, New Hampshire, New Jersey, New York, Rhode Island, Vermont, and Virginia, set at 75 million short tons in 2021 and decreases by 2.275 million tons per year until 2030 [101].

In addition, the Inflation Reduction Act of 2022 (IRA) is included in PyPSA-USA, including the Production Tax Credit (PTC) and the Investment Tax Credit (ITC) for clean electricity [102]. Under IRA, eligible clean electricity projects can select whether to take the PTC or

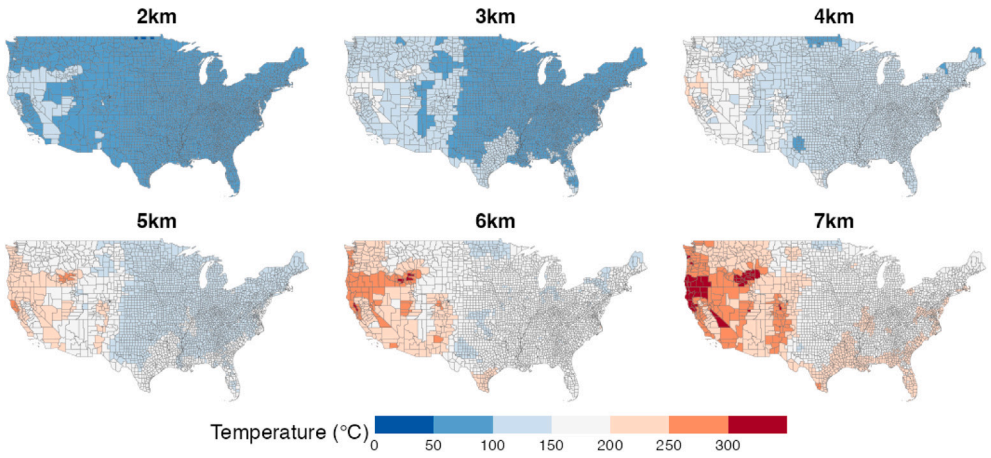

Fig. 3. Subsurface temperature from [104] from 2 to 7 km underground.

the ITC. For PTC, we assigned a $27.50/MWh for onshore wind, solar, and biomass; and for ITC, a 30% tax credit would be applied to offshore wind, geothermal, SMR, and all storage systems. However, to account for the potential repeal of Inflation Reduction Act (IRA) incentives for clean energy projects, we include sensitivity scenarios excluding these incentives Appendix F.

2.2. Geothermal resources

2.2.1. Underground resources

The temperature-at-depth profiles for the conterminous United States (CONUS) were extracted from Aljubran and Horne [103,104], who utilized a physics-informed graph neural network to generate detailed national temperature-at-depth maps. The data were then georeferenced and aggregated to the county-level. These profiles show higher temperatures in the Eastern and Western United States compared to earlier maps from Southern Methodist University (SMU; [105]), particularly at depths exceeding four kilometers (Fig. 3). It indicates that in most regions, for a given target temperature, geothermal resources can be accessed at shallower depths and thus lower drilling costs than previously thought. A detailed comparison of surface temperatures between the SMU products and Aljubran and Horne [104] is provided in Appendix C.

While previous studies indicate that depths of 3–5 km are the most viable for deep geothermal resource exploitation due to favorable technical and economic feasibility, deeper resources within the 5–7 km range are considered technically achievable despite of less economically attractive [2,106]. The geothermal potential per volume underground follows the method of [9].

2.2.2. Supply curves

In this study, we use an open-source model, GEOthermal energy for Production of Heat and electricity (“IR”) Economically Simulated (GEOPHIRES-X; [67,107]), to estimate supply curves for both power generation via EGS and DDU for heating. GEOPHIRES combines reservoir, wellbore, and surface plant technical models with cost correlations and levelized cost models to estimate the capital and operation and maintenance costs, instantaneous and lifetime energy production, and overall levelized cost of energy of a geothermal plant. In addition to electricity generation, direct-use heat applications and combined heat and power or cogeneration can be modeled.

Our previous study used the Geothermal Electricity Technology Evaluation Model (GETEM) and QUE$TOR to estimate the EGS supply curve [9]. We choose GEOPHIRES-X here because it was developed based on GETEM and recent publications. GEOPHIRES-X is updated regularly to reflect recent technological advances, including well drilling and completion cost reduction, well flow rate increase, and surface plant cost adjustment. GEOPHIRES-X assumed a multiple fracture reservoir model [107,108], with Ramey’s wellbore heat transmission model [109] applied to simulate heat losses in the production wellbore. Additionally, GEOPHIRES-X is developed in Python, a widely-used programming language, enabling greater flexibility and customization for users.

We use drilling cost data reported by Fervo Energy from its Project Cape in southwest Utah [68] to help us determine which cost curve to use from the literature. As experience accumulated, drilling times fell 70% compared to their first horizontal well at Project Red in 2022 [110]. Assuming the same lateral length of 1500 m as used by Fervo, this increased efficiency led to substantial cost reductions, with drilling costs for the first four horizontal wells decreasing from $9.4 million (*Before*) to $4.8 million (*After*) per well. In Fig. 4, we compare the updated drilling costs with four well-cost curve scenarios for Large Diameter and Horizontal Liner wells - 1) Business-as-Usual (*BAU*), 2) Intermediate 1 (*Int 1*), 3) Intermediate 2 (*Int 2*), and 4) *Ideal* - from four scenarios in Lowry et al. [111]. The previous 500 m lateral length was extrapolated to 1500 m for consistent comparison. Fig. 4 also shows our prior estimates based on the QUE$TOR model [9]. This comparison shows that the latest drilling cost estimation (*After*) falls substantially below our prior estimates from QUE$TOR and slightly below the lowest (*Ideal*) cost curve from Lowry when the latter were adjusted for lateral drilling length (Fig. 4). Thus, we choose the Ideal curve from Lowry with the adjusted lateral drilling costs as the drilling cost baseline for this study. In addition, we increased the flow rate from 80 kg/s used in the previous study to 107 kg/s, aligning with the maximum flow rate reported from Fervo’s Project Red [112]. The model assumes a 100% drilling success rate and thus neglects the costs of unsuccessful wells.

GEOPHIRES-X was also used to compute the supply curves for DDU systems, following the examples in Beckers et al. [67] and Tester et al. [113]. These studies modeled direct-use heating using the Multiple Parallel Fractures Model, similar to the approach for EGS, simulating a reservoir at a 2.8-km depth based on conditions at the Cornell University Borehole Observatory (CUBO), which is designed to provide consistent district heating for the campus. The system included one production well and one injection well, each with a 7-inch diameter and a flow rate of 40 kg/s, while maintaining a reinjection temperature of 30 °C. Next, we replaced the drilling and completion costs with the Ideal curve from Fig. 4.

The model iterated through all combinations of depth and resource temperature, gathering techno-economic data outputs for both EGS and DDU, including average production (MW), average production temperature (° C), overnight capital costs ($) (including the costs for exploration, stimulation, field gathering system, surface equipment, drilling and completion, and surface plant), and annual O&M costs ($/year),

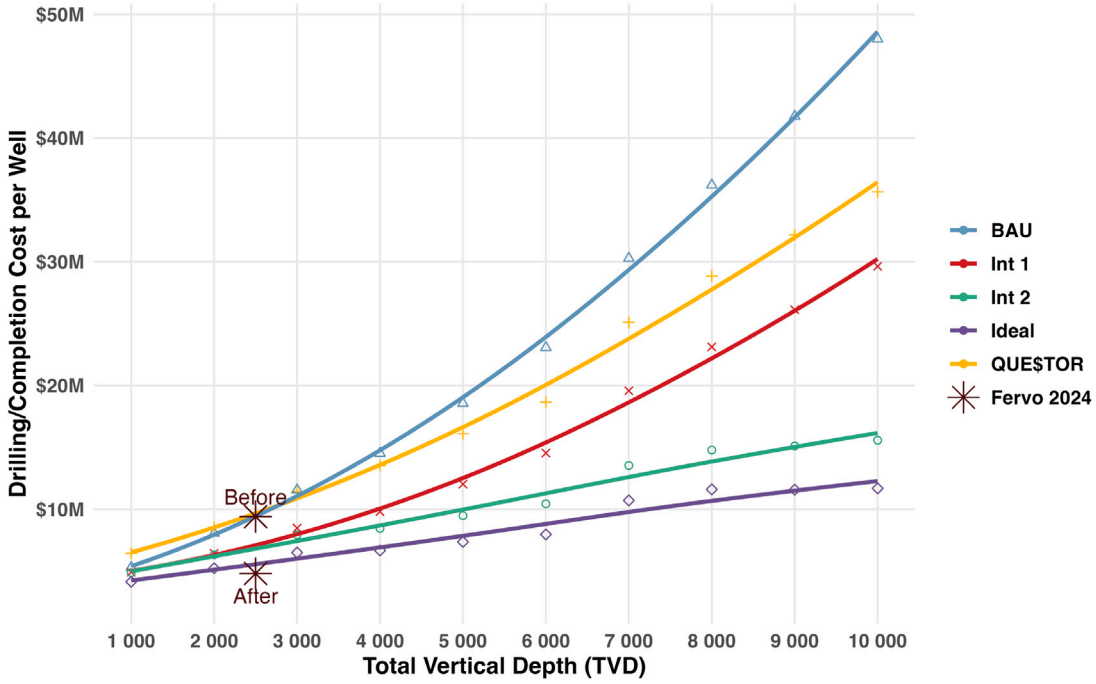

Fig. 4. Drilling costs of geothermal wells comparing four drilling scenarios (*BAU*, *Int1*, *Int2*, *Ideal*) under [111], QUE$TOR curves from Chen et al. [9], and Fervo's estimation in 2022 (*Before*) and 2024 (*After*) [68]. All cost estimates assume a lateral length of 1500 m.

which were used to calculate capital expenditures (CapEx; $/MW) and FOM ($/MW/year). The annualized CapEx was estimated internally using PyPSA-USA, assuming a 30-year lifetime and a weighted average cost of capital of 5% per year [82].

For integration into PyPSA-USA, county-level geothermal resource assessments from GEOPHIRES-X were processed differently for electricity (EGS) and industrial heating (DDU). For EGS, county-level supply curves were developed and aggregated to balancing areas, with resources classified by temperature and depth; higher-quality resources with hotter subsurface temperatures at shallower depths were associated with lower CapEx and FOM costs, which were then provided as inputs to PyPSA-USA to build future new EGS capacity. For DDU, county-level IPH demand data were matched with averaged temperature-at-depth profiles, allowing direct comparison of required process heat temperatures (demand) with the maximum geothermal temperatures available at the shallowest feasible depths (supply), where drilling costs are minimized. In cases where the geothermal resource temperature exceeded the IPH requirement, the lowest CapEx and FOM costs from GEOPHIRES-X were used as model inputs to build new heating facilities using DDU.

The capacity of EGS is subjected to ambient temperature as noted in prior studies [10,114]. Thus, we applied a varying capacity factor multiplier to the nameplate capacity based on ambient temperature collected from Atlite Appendix D.

3. Results

3.1. EGS and DDU supply curves

Fig. 5 compares the CapEx of the cheapest 1000 GW_e of geothermal resources for EGS between this study and our previous analysis [9], which included one 2023 Business-as-Usual (BAU) and two future CapEx scenarios for 2035. The BAU scenario from Chen et al. [9], based on late 2022 estimates, indicated significantly higher CapEx, ranging from $7000 to $16,000 per kW. In this study, due to the substantial reductions in drilling costs and increased flow rates during the 2024 operation reported by Fervo, CapEx estimates are notably lower, ranging from $3500 to $6000 per kW, based on GEOPHIRES-X calculations. This estimation falls below the Moderate cost reduction scenario and is only marginally higher than the Advanced scenario in 2035, suggesting a faster-than-expected learning curve for EGS deployment in the last few years.

GEOPHIRES estimates the CapEx for geothermal DDU systems, as shown in Fig. 5, illustrating a strong correlation between CapEx, depth, and reservoir temperature. The CapEx varies from $588 to $3000 per kWth and the corresponding Levelized Cost of Heat (LCOH) is estimated between $11.6 and $48 per MWh. Annual operation and maintenance (O&M) costs are projected to range from $0.37 million to $1.65 million.

Based on our estimates of CapEx (Fig. 6) and subsurface resources (Fig. 3), geothermal DDU technology can effectively supply heating for temperatures up to 275 °C. Based on that temperature threshold, geothermal DDU has the maximum potential to replace over 205 TWh of annual IPH demand currently met by fossil fuels, accounting for about 26.5% of today's total IPH. This substitution could save an estimated 7 million metric tons of coal, 14.3 billion cubic meters of natural gas, and 125 million liters of heating oil annually, translating to a CO_2 emissions reduction of nearly 46 million metric tons per year.

Industries with the highest geothermal DDU potential include alkali and chlorine manufacturing, wet corn milling, petroleum refineries, and paper/paperboard mills, each with fossil fuel demand over 28 TWh annually. The greatest DDU potential (160 TWh per year) falls within the 150–200 °C range, as most industrial sites have sufficient underground resources at these temperatures. For demands above 220 °C, geothermal can only meet about 1 TWh annually based on our analysis.

Regionally, Texas and Louisiana hold the highest technical potential for transitioning from fossil fuels to geothermal DDU, especially in alkali and chlorine manufacturing and petroleum refineries, with over 28 TWh in annual demand, according to McMillan and Ruth [40]. Iowa and Illinois follow, where low-temperature geothermal can serve wet corn milling for nearly 20 TWh heating demand.

Building all the potential DDU sites would require an estimated capital cost of $181 billion. Over a 30-year lifetime, the average LCOH would be under $16/MWh, decreasing as temperature of geothermal resource increases. For temperatures above 250 °C, the average LCOH is $13.4/MWh.

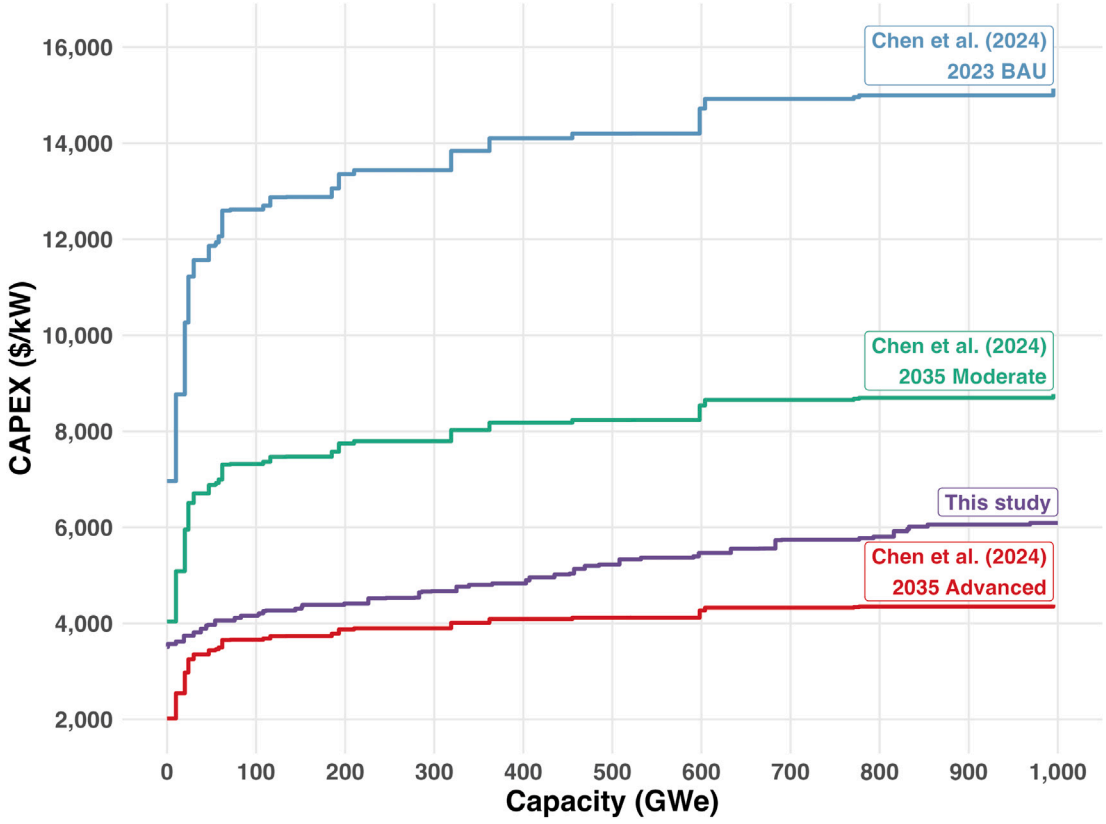

Fig. 5. Comparison of deep EGS resource supply curves for the least-cost 1000 GW_e from this study with three scenarios from Chen et al. [9], the BAU scenario in 2023 and two future scenarios, *Moderate* and *Advanced*, projecting the costs in 2035.

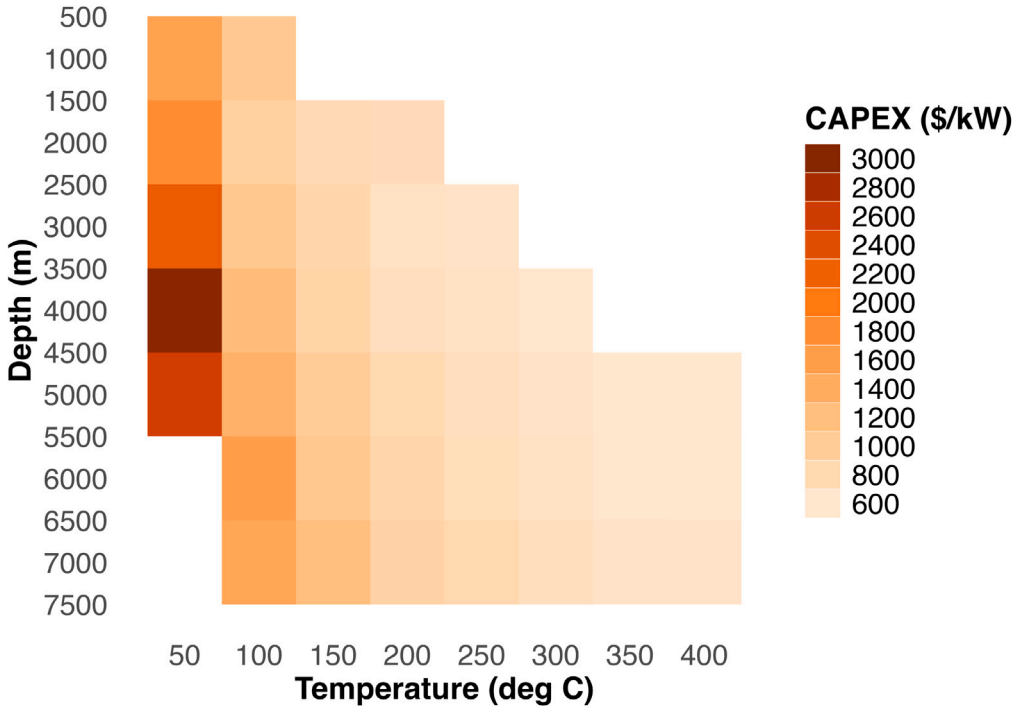

Fig. 6. CapEx estimation ($/$kW_{th}$) of geothermal DDU for all potential depths and temperatures.

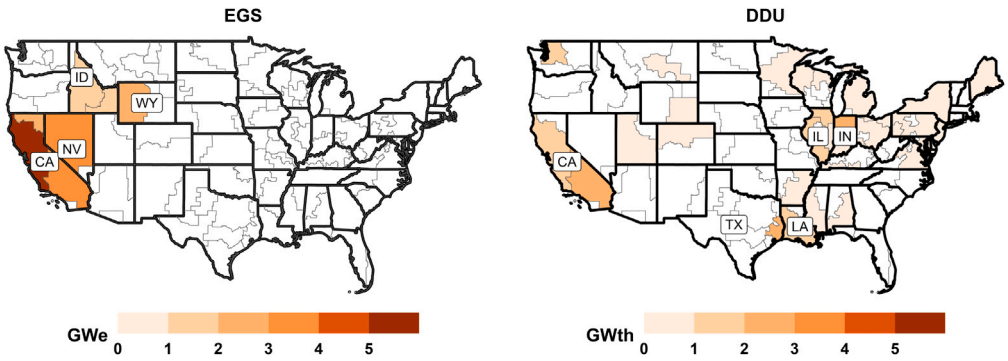

Fig. 7. Cost-minimizing EGS and DDU capacity (GW_e and GW_{th}) by balancing areas in the CONUS.

3.2. PyPSA results

3.2.1. Overall geothermal economic potential

Cost-minimizing EGS and DDU deployments are displayed in Fig. 7. The model finds that systemwide costs could be minimized by developing EGS in Western states including California, Oregon, Idaho, Nevada, Colorado, and Wyoming with a combined capacity of 40.0 GW_e. California alone is expected to contribute more than half of this total, driven by its substantial electricity demand, high reserve margin requirement for the WECC, and high-quality geothermal resources. More broadly, Western states dominate EGS deployment because of their favorable geologic conditions, including higher geothermal gradients and accessible deep reservoirs, which reduce drilling costs and improve economic competitiveness relative to other generation technologies. The results indicate that even at current CapEx estimates, EGS can effectively compete with other power generation technologies in specific states. Our analysis does not consider complications related to permitting, regulation, and construction duration.

In parallel, cost-minimizing deployments of geothermal DDU are more geographically diverse, featuring industrialized regions of California, Texas, Louisiana, Illinois, and Indiana among a national total of 30.1 GW_{th}, where applicable industrial heat demand is especially high in sectors such as petroleum refining, petrochemical manufacturing, and pulp and paper. The details of power and heating sectors are analyzed in the following subsections.

3.2.2. Power system

Fig. 8 compares the optimized power generation capacity in 2030 to actual 2023 levels. The model identifies a significant amount of retirements of fossil fuel plants that would reduce systemwide costs due to their high fuel costs. Coal-fired power plants would see notable phase-outs, with 39.4 and 19.5 GW_e retired in the Eastern and Western regions, respectively, while ERCOT would retain its existing coal plants to ensure the reserve margin requirement. Additional CCGT and OCGT would be built to ensure the reserve margin requirements, totaling 15.7 and 140 GW_e across CONUS.

On the other hand, renewable energy sources would experience substantial growth. Systemwide costs could be minimized by increasing solar capacity from 91.4 GW_e in 2023 to 159.3 GW_e in 2030, with significant additions in Texas, Florida, and California. Wind capacity would grow by 87.8 GW_e, with New Mexico, Indiana, Ohio, and Wisconsin leading in new wind farm deployments.

Under existing carbon policies and without further technology cost reductions, systemwide costs could be minimized by deploying 40 GW_e of EGS, predominantly in five Western states: California (22.7 GW_e), Wyoming (4.3 GW_e), Nevada (3.3 GW_e), Idaho (3.1 GW_e), and Colorado (1.1 GW_e). This capacity estimate significantly exceeds previous studies [9], which projected limited EGS development unless aggressive cost reductions or stringent carbon policies were implemented.

Fig. 9 illustrates the average generation profiles across ERCOT, Western, and Eastern Interconnects for all plant types. In WECC, over 50% of electricity would come from low or zero carbon emitting sources, with periods — such as afternoons and midnights in spring, fall, and winter — reaching over 90%. Geothermal energy would account for 15%–40% of the total electricity supply in this region. Particularly, new EGS are expected to generate 115 TWh of clean electricity annually in WECC. Based on the 2023 eGRID CO_2 emission rate of 385 kg/MWh [115], this would result in approximately 120.7 Mt of avoided CO_2 emissions.

3.2.3. Industrial heating

Our cost-minimization modeling reveals significant potential for both electrification and geothermal DDU to supply industrial heat, emphasizing the trade-offs among geothermal resource availability, renewable energy integration, fuel prices, and the need to meet specific temperature requirements for industrial processes. Fig. 10 shows that geothermal DDU becomes an attractive option for industrial heating needs within the 100–200 °C range, potentially enabling the deployment of 29.1 GW_{th} of capacity. Although the opportunities for geothermal DDU above 200 °C are more limited, they still exist in areas with high-quality geothermal resources located in Western U.S. states.

By industrial NAICS subsector, petroleum refineries and iron/steel mills exhibit the greatest potential for geothermal DDU, with an estimated 18.9 GW_{th} and 4.8 GW_{th}, respectively, to supply the low-temperature IPH. Petroleum refineries demand substantial amounts of heat below 200 °C, and many are located in California, Louisiana, and Texas—regions with high geothermal resource quality (Fig. 11). Additional sectors such as petrochemical manufacturing, alkali and chlorine manufacturing, and paper mills could each utilize over 1 GW_{th} of geothermal DDU.

The current fossil fuel-based heating, coal and gas-fired IPH supply can be largely substituted with geothermal DDU, heat pumps, and resistance heaters (Fig. 12). In total, 66% of coal, 46% of gas, and nearly 100% of oil-based heating generation would be substituted by electrification or geothermal options, delivering 670 TWh of annual IPH supply—equivalent to 47% of total heating demand. Especially at lower temperature ranges, clean heating solutions would provide 58% of annual heating, primarily from geothermal DDU. For higher temperature needs above 200 °C — where geothermal DDU would require deeper drilling and heat pumps are ineffective — resistance heaters become a competitive option for industries such as petroleum refineries, ethyl alcohol production, lime manufacturing, nitrogenous fertilizer production, and pulp mills. The shift to electric heating in these sectors would be most favorable in regions where natural gas prices are high or where electricity costs are reduced by the growth of renewable energy generation Appendix E.

Comparing two electric heating options, industrial heat pumps and resistance heaters, industrial heat pumps are only capable of supplying heat below 180 °C. As a result, heat pumps dominate IPH supply when

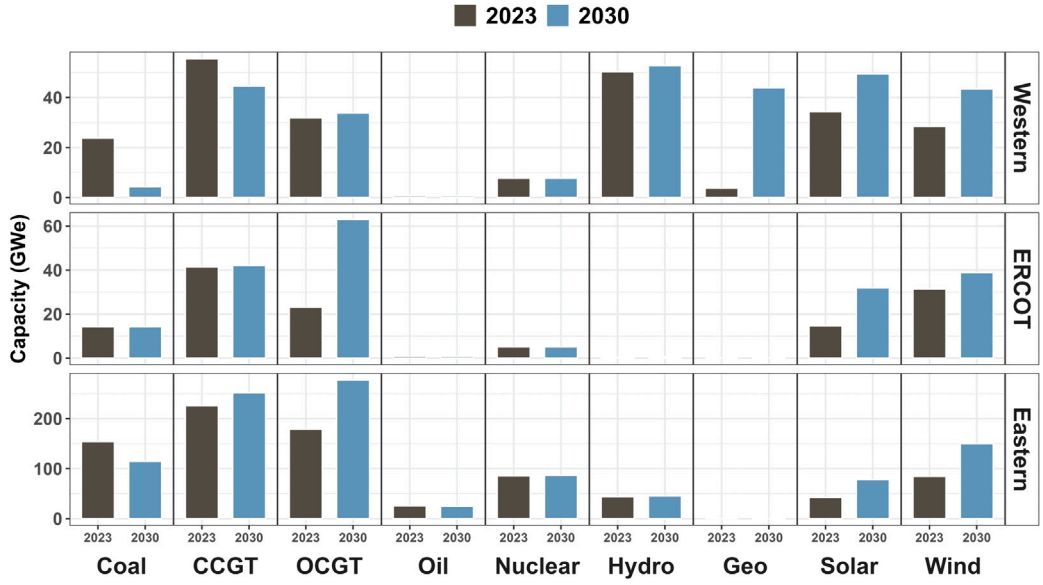

Fig. 8. Power plant capacities (GW_e) in 2023 and the capacities modeled to minimize system costs in 2030.

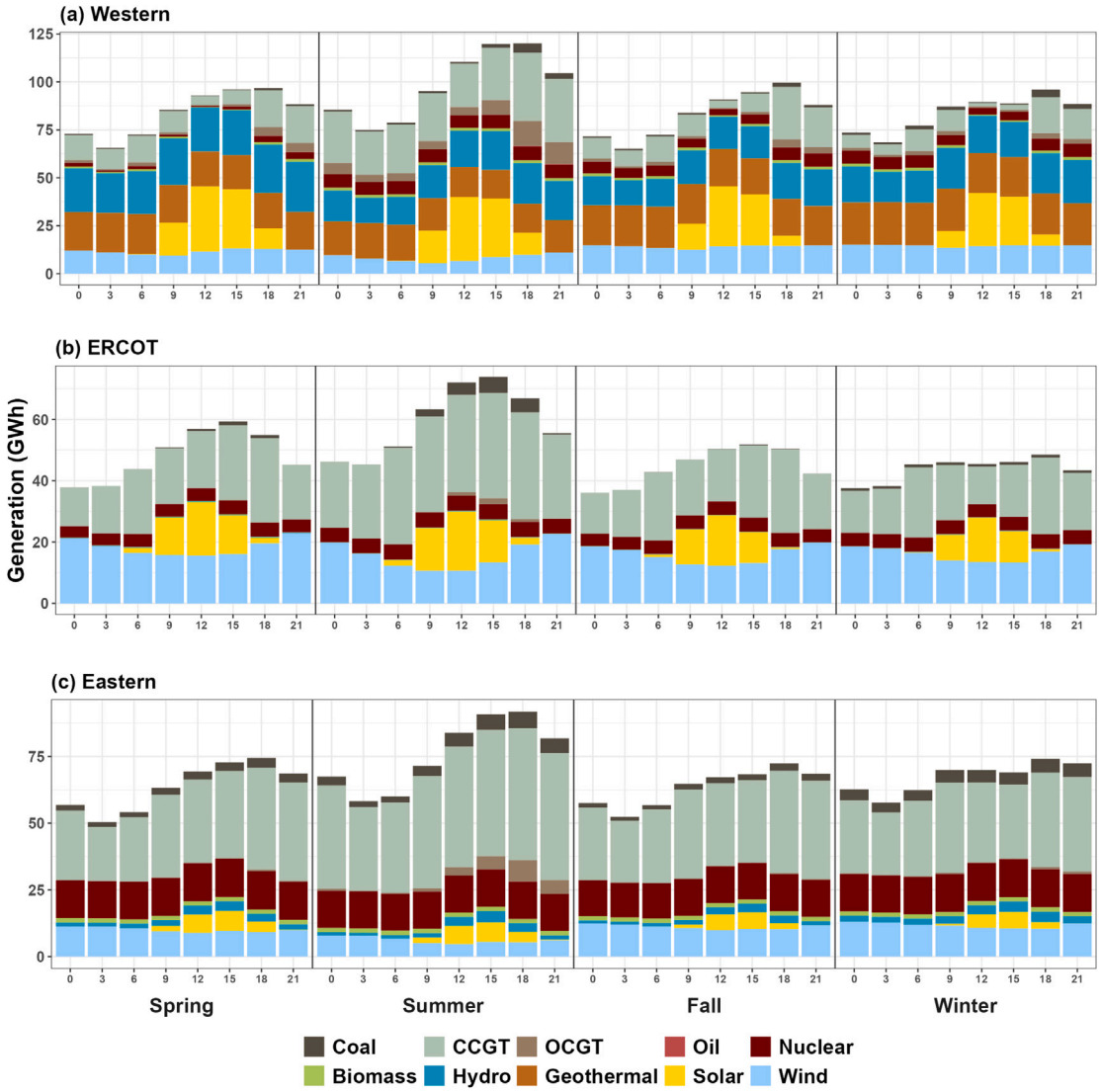

Fig. 9. Generation dispatch by fuel types in (a) the Western Interconnect, (b) ERCOT, and (c) the Eastern Interconnect, averaged by hour and season.

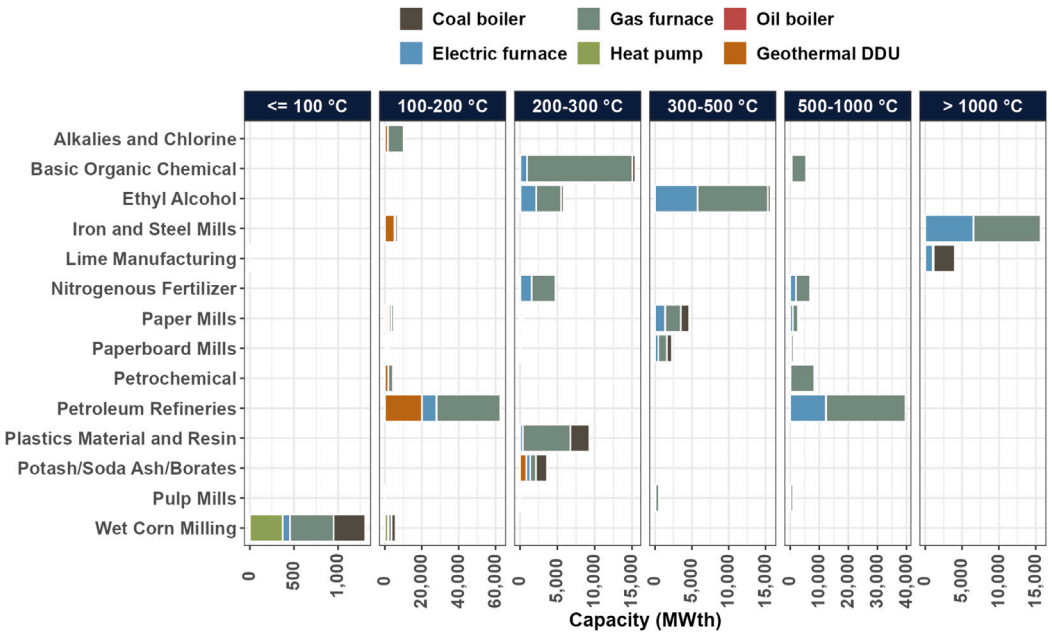

Fig. 10. Distribution of industrial heating capacity (MW_{th}) by temperature range and technology type across all industrial sectors.

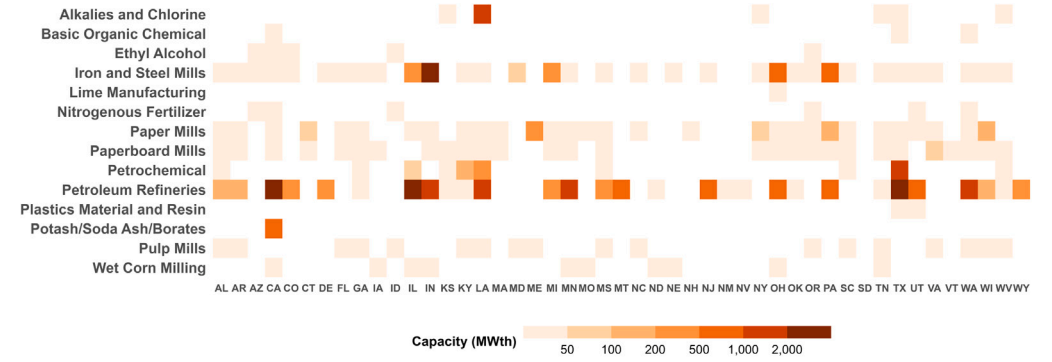

Fig. 11. Geothermal DDU capacity distribution (MW) by NAICS subsector and U.S. state in a cost-minimizing simulation.

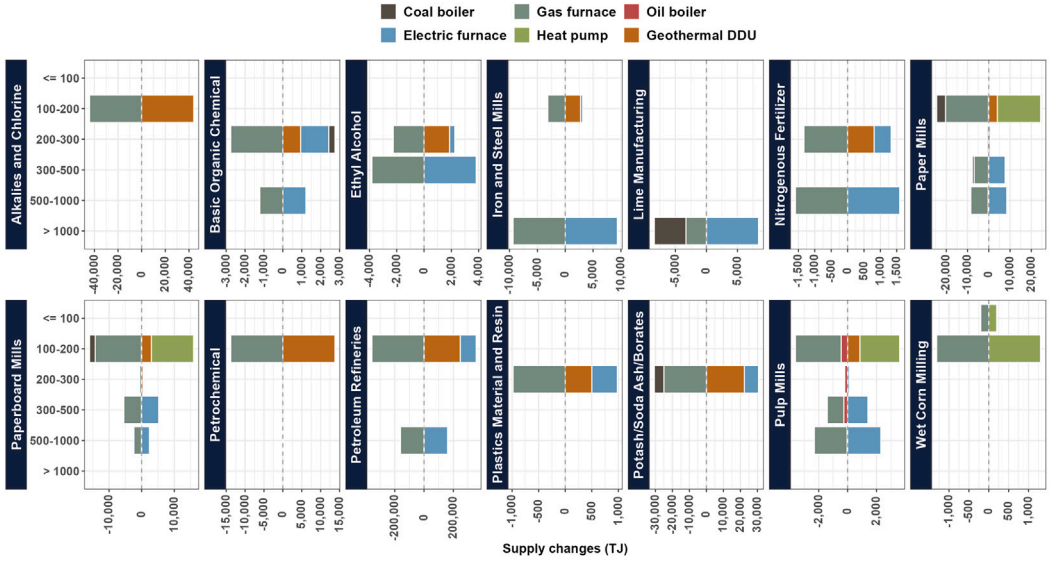

Fig. 12. Cost-minimizing changes in IPH supply, showing the transition from fossil fuel-based systems (coal, gas, oil boilers) to cleaner heating technologies (resistance heaters, heat pumps, geothermal DDU) across major industrial sectors. Positive values indicate increased adoption of clean heating options, while negative values represent reduced use of traditional fossil fuels.

the required temperature is below the threshold where geothermal resources are less favorable. However, in northern states like Iowa, Illinois, Michigan, and Nebraska, where heat pump efficiency fluctuates significantly during cold weather, resistance heaters are also deployed to supplement low-temperature demand and compensate for variations in heat pump performance.

The model estimates significant reductions in CO_2 emissions across various NAICS industrial subsectors when switching from conventional fossil fuels supply. Notable reductions include 95% for wet corn milling, 94% for potash/soda ash/borates manufacturing, 78% for iron and steel mills, and 70% for paper mills. Other industries such as petrochemicals, alkali and chlorine manufacturing, lime manufacturing, pulp mills, ethyl alcohol, petroleum refineries, paperboard mills, and potash/soda ash/borates could also achieve reductions of over 50%, while other sectors show only modest reductions due to limited opportunities for electrification or geothermal DDU adoption. Categorized by temperature ranges, the most significant CO_2 reductions occur below 100 °C and in the 100–200 °C range, with decreases of 95% and 74%, respectively, compared to the current baseline. Moderate reductions are seen for processes above 300 °C.

3.2.4. Sensitivity analysis

We analyzed the sensitivity of results to assumed natural gas prices, which are highly volatile and influenced by weather and geopolitical factors. Our sensitivity analysis focused on natural gas prices that could influence geothermal deployment in ERCOT and WECC—regions with both high natural gas price volatility and high-quality geothermal resources. To assess the model sensitivity, we applied three price adjustment factors to 2023 natural gas prices: a 50% reduction, a 50% increase, and a doubling of the price. Additionally, we examined a nationwide natural gas price scenario based on the EIA Annual Energy Outlook (AEO) 2023 [98], which projects an industrial natural gas price of $4.19 per MMBTU in 2030, applied uniformly across all states and all hours.

In WECC, halving the natural gas price would double the industrial heating capacity of gas boilers and lead to the construction of an additional 1.5 GW_e of OCGT (Fig. E.2). For geothermal, this lower gas price scenario would result in 0.6 GW_{th} less geothermal DDU capacity and nearly 30 GW_e less EGS plant capacity, indicating that EGS is much more sensitive to natural gas price changes than DDU. The impact on wind and solar would be comparatively smaller, with 8.9 GW_e less wind capacity and a negligible reduction in solar capacity.

Historically, natural gas prices in ERCOT are much lower than in WECC due to Texas's abundant local production, proximity to supply sources, and well-developed infrastructure, which minimize transportation and delivery costs. However, the model shows high sensitivity to gas price variations in ERCOT (Fig. E.3). For example, a 50% increase in gas prices would favor geothermal DDU systems over industrial gas boilers. Higher gas prices also favor the adoption of resistance heaters. If gas prices were to double, substantial EGS deployment would become cost-minimizing, with capacity reaching up to 5.5 GW_e. Additionally, wind capacity would expand in response to rising fossil fuel costs, increasing by 19% under a 50% gas price increase and by 26% if gas prices doubled.

Finally, if a uniform natural gas price were applied in the model, states such as Louisiana and Texas — where historical gas prices have been low — would show a high potential for transitioning from gas boilers to geothermal DDU or electrification options if prices were to rise (Figs. E.4 and E.5).

To assess the impact of a potential repeal of the IRA, we also conducted a sensitivity analysis comparing scenarios with and without IRA incentives. Without the IRA, wind deployment declines across all regions, and nearly half of projected geothermal EGS capacity in WECC would not be built due to increased capital costs. This gap is filled by additional fossil generation, including 17.4 GW_e and 14.2 GW_e of new CCGT in the East and West Interconnections, respectively. Also in the No IRA scenarios, reported higher electricity prices due to a repeal of incentives also reduce electrification of industrial heating, resulting in 13.8 GW_{th} less resistance heating and 0.3 GW_{th} less heat pump capacity. However, geothermal DDU becomes slightly more competitive, increasing by 3.2 GW_{th}, and coal boiler use rises by 17.4%. Overall, the loss of IRA incentives would hinder clean technology deployment, increase fossil fuel reliance, and raise emissions. Nationwide CO_2 emissions would rise by 166.2 Mt, delaying national decarbonization progress. Detailed modeling results comparing two scenarios are provided in Appendix F.

4. Discussion

This study highlights the significant opportunities for geothermal energy in the United States that could emerge in the 2030s, driven by steep declines in drilling costs. The model estimates that a total of 40 GW_e of EGS deployment, mainly in Western states like California, would minimize system costs. Geothermal DDU is found to be cost-minimizing in certain industries requiring 100–300 °C heat where subsurface conditions are favorable. Key industrial NAICS subsectors that require low-temperature heat such as petroleum refineries, iron and steel mills, petrochemicals, alkali and chlorine, and paper mills are the leading candidates for adopting DDU. In these subsectors, DDU also competes with resistance heaters and heat pumps, particularly for regions where renewable-sourced energy is abundant. As a result, the wide adoption of geothermal energy and other power-to-heat technologies could lead to substantial CO_2 reductions, up to 85% in certain NAICS subsectors.

Compared to our previous estimation [9], where we projected EGS would only be built under aggressive cost reductions or high CO_2 reduction requirements, this study finds that EGS could already be cost-competitive with existing plant types and policies, particularly in regions with high-quality subsurface resources and high natural gas prices. Other studies have estimated that geothermal capacity in the United States could range from 11 to 150 GW_e by 2050 [10,11,116,117]. Our study indicates a strong potential to reach the higher end of these projections if costs continue to decrease. While these studies primarily focus on geothermal for power generation, research on geothermal DDU remains highly limited, which suggests the need for future studies on industrial and other direct-use applications.

As for heating, IPH is for now supplied predominantly by fossil fuels, contributing significantly to carbon emissions. This study found that over 60% of IPH demand, approximately 844 TWh annually, requires temperatures below 300 °C, and up to 209 TWh of geothermal DDU systems could technically replace 24.5% of this demand. The model estimates that costs could be minimized by deploying 31 GW_{th} of geothermal DDU in areas where low-temperature demand aligns with high-quality geothermal resources. Targeted policies focused on reducing carbon emissions in industrial heating could drive the adoption of geothermal DDU and other low-carbon technologies.

Fuel costs, particularly for natural gas, significantly affect the competitiveness of geothermal technologies. High gas prices favor EGS and DDU by making them cost-competitive for baseload power and industrial heating, especially in volatile markets. Policy changes, geopolitics, and market factors all significantly impact natural gas prices, adding uncertainty to future costs of natural gas electricity and heat.

An important caveat to our results is that the model assumes geothermal resources can be utilized where temperatures are favorable. Real-world site selection is more complex, requiring seismic risk assessments, environmental impact statements, permitting and regulatory challenges, and addressing public concerns. These factors make the actual development and implementation of EGS and DDU systems significantly more challenging than suggested by the model.

This study has several limitations. For the power sector, it focuses primarily on EGS deployment while excluding potential contributions

from traditional hydrothermal systems, AGS, and single-well geothermal systems. AGS and single-well technologies could offer additional pathways to harness deep geothermal resources [15,16,118,119]. However, performance and cost data for these emerging technologies remain limited relative to EGS, and thus they were not included in this analysis. Future studies should consider their inclusion as data availability improves, since their different design characteristics may broaden geographic applicability.

For industrial heat, renewable options are limited to geothermal DDU and two electrification technologies, neglecting other clean energy solutions such as combined heat and power (CHP), biomass, and concentrating solar-thermal power (CSP). Also, the analysis may oversimplify the diversity and complexity of industrial heating technologies, spatial distribution, and operational practices, which influence fuel choice under specific circumstances. Furthermore, since the DDU supply curves are aggregated by balancing authorities, the geothermal deployment cost estimates may not accurately reflect site-specific geological variability or unforeseen drilling challenges.

Additional modeling limitations include reliance on a single representative historical year and assumptions of perfect foresight optimization and market conditions, rather than a myopic decision-making process like ReEDS. The model selects the most cost-effective solutions over the planning horizon without accounting for real-world constraints such as phased investment decisions, technology learning curves, or market uncertainties. As a result, PyPSA-USA assumes immediate access to identified resources and infrastructure while ignoring project development timelines, permitting delays, or geothermal exploration risks, potentially overestimating near-term EGS and DDU deployment. In practice, EGS projects are expected to face lengthy permitting and development cycles (typically 5–7 years; [120]), which could delay realization of capacity relative to modeled outputs. Also, with few established players in the industry, capital and human resource limitations may constrain the pace of deployment. Other factors like policy shift, supply chain constraints, workforce availability, and public acceptance could also impact geothermal adoption.

In the sector-coupled model, electricity and industrial heating systems are jointly optimized, enabling cross-sector considerations to shape deployment patterns. Deployment in one sector influences capacity requirements and utilization in the other. The framework could be further expanded to include additional sectors, including residential and commercial buildings and green hydrogen production. Incorporating these sectors in future studies would provide further insights for energy systems planning.

Overall, PyPSA-USA serves as a valuable tool for forecasting energy system expansion under varying market dynamics. However, caution should be taken when interpreting results, as capacity expansion models inherently simplify assumptions about energy system behavior and the technical characteristics of power and heating generation technologies.

5. Conclusion

This study demonstrates the growing potential for geothermal energy to contribute significantly to the decarbonization of the U.S. energy system. Through integrated modeling that combines capacity expansion, sector coupling, we find that recent reductions in drilling costs and favorable subsurface conditions could enable geothermal technologies to become cost-competitive in the near future. Our models project up to 40 GW_e of EGS and 31 GW_{th} of DDU could be deployed cost-effectively, primarily in Western states and in industrial sectors with low- to medium-temperature heat demands.

Despite these promising outcomes, the results remain subject to significant uncertainties, particularly in cost projections, subsurface resource characterization, and real-world deployment feasibility. The model employed simplified assumptions and focused solely on cost-optimized solutions, without accounting for practical constraints such as site-specific geological variability, seismic risk assessments, environmental and social impacts, permitting and regulatory hurdles, and public acceptance. These factors can substantially influence the viability and pace of geothermal development. Therefore, high-level techno-economic modeling should be complemented by detailed planning studies and site-specific assessments to better guide strategic geothermal deployment and policy design.

Our sensitivity analysis highlights the critical role for policy to support geothermal development. Adverse changes in policy could slow deployment, increase reliance on fossil fuels, and delay decarbonization. Targeted policy measures that address long permitting, regulatory, and exploration timelines would further enable more strategic and timely deployment of geothermal resources.

CRediT authorship contribution statement

Chen Chen: Writing – review & editing, Writing – original draft, Visualization, Validation, Methodology, Investigation, Formal analysis, Conceptualization. **Daniel S. Cohan:** Writing – review & editing, Supervision, Methodology, Investigation, Funding acquisition, Conceptualization.

Declaration of competing interest

The authors declare the following financial interests/personal relationships which may be considered as potential competing interests: Daniel Cohan reports financial support was provided by Project Innerspace. If there are other authors, they declare that they have no known competing financial interests or personal relationships that could have appeared to influence the work reported in this paper.

Acknowledgment

Funding for this research was provided by Project Innerspace. The authors declare that there is no conflict of interest and no other financial support.

Appendix A. Optimization formulations

$$\min_{p,h,s,p_h,h_s} \quad \sum_t \omega_t \left[\sum_g g_{0,g,t} \cdot p_{g,t} + \sum_h h_{0,h,t} \cdot h_{g,t} + \sum_s o_{0,s,t} \cdot s_{s,t} + \sum_g F_{g,t} \cdot p_{g,t} + \sum_h F_{h,t} \cdot h_{g,t} \right] + \sum_g M_g \cdot \bar{p}_g + \sum_h M_h \cdot \bar{h}_g + \sum_s M_s \cdot \bar{s}_s + \sum_g C_g \cdot p_{\text{new},g} + \sum_h C_h \cdot h_{\text{new},g} + \sum_s C_s \cdot s_{\text{new},s} \tag{A.1}$$

s.t.

$$p_{g,t}^{\min} \le p_{g,t} \le p_{g,t}^{\max}, \quad \forall t \in T, g \in G \tag{A.2}$$

$$\bar{p}_g \le \bar{p}_g^{\max}, \quad \bar{h}_g \le \bar{h}_g^{\max} \tag{A.3}$$

$$0 \le S_{s,t}^{\text{out}} \le S_s^{\bar{S}}, \quad 0 \le S_{s,t}^{\text{in}} \le S_s^{\bar{S}}, \quad \forall s \in S, t \in T \tag{A.4}$$

$$SOC_{s,t} = SOC_{s,t-1} + \eta_s^{\text{in}} S_{s,t}^{\text{in}} - \eta_s^{\text{out}} S_{s,t}^{\text{out}}, \quad \forall s \in S, t \in T \tag{A.5}$$

$$f_{b,t}^{\min} b_t \le f_{b,t} \le f_{b,t}^{\max}, \quad \forall b \in B, t \in T \tag{A.6}$$

$$\sum_g p_{g,t,n} + \sum_s S_{s,t,n}^{\text{out}} - \sum_s S_{s,t}^{\text{out}} - \sum_s S_{s,t}^{\text{out}} - \sum_s K_{b,t} f_{b,t} + \sum_h h_{g,t,n}^{\text{elec}} = DP_{t,n}, \quad \forall n \in N, t \in T \tag{A.7}$$

Table B.1
Annual demand (TJ) and CO_2 emissions (MT) for all industries by NAICS code.

NAICS	Description	Demand (TJ)	CO_2 (MT)	Gas (TJ)	Coal (TJ)	Oil (TJ)	Top States
212391	Potash/Soda Ash/Borates	81,805	6.1	34,110	24	47,671	CA, NM, WY
311221	Wet Corn Milling	186,189	14.5	60,912	0	125,277	IA, IL, NE
322110	Pulp Mills	137,069	10.9	37,928	3,566	0	FL, GA, NC
322121	Paper Mills	452,727	34.7	181,889	5,952	92,136	AL, ME, WI
322130	Paperboard Mills	284,224	21.9	94,109	939	40,419	GA, LA, VA
324110	Petroleum Refineries	2,213,752	121.8	2,205,758	7,345	627	CA, LA, TX
325110	Petrochemical	275,063	15.0	274,964	0	0	IL, LA, TX
325181	Alkalies and Chlorine	231,651	12.0	223,670	0	7,981	LA, TX, WV
325193	Ethyl Alcohol	312,150	16.4	294,516	0	14,925	IA, IL, NE
325199	Basic Organic Chemical	424,960	22.5	413,525	0	9,665	AL, LA, TX
325211	Plastics Material/Resin	207,707	13.0	145,359	0	61,325	LA, TN, TX
325311	Nitrogenous Fertilizer	171,939	8.9	171,939	0	0	LA, ND, OK
327410	Lime Manufacturing	94,127	8.3	7,173	53	86,901	KY, MO, OH
331111	Iron and Steel Mills	437,552	49.6	437,506	34	7	IN, OH, PA

$$\sum_{h} h^{\text{out}}_{g,t,n} + \sum_{h} h^{\text{elec}}_{g,t,n} = DH_{t,n}, \quad \forall n \in N, t \in T \tag{A.8}$$

$$\sum_{q} h^{\text{fuel}}_{g,t,n} \cdot \eta^{\text{fuel}}_{g,t,n} = \sum_{s} h^{\text{out}}_{g,t,n}, \quad \forall n \in N, t \in T, g \in H \quad \text{[fossil/geo only]} \tag{A.9}$$

$$\sum_{d} Y_d \bar{p}_d \geq \max_{t}\left(\sum_{n} DP_{t,n}\right)(1 + PRM) \tag{A.10}$$

$$\sum_{L}\sum_{d} e_d p_{d,t} \leq E \tag{A.11}$$

Sets:

- T: Set of time periods (only 2030 in this study).
- G: Set of power generation units.
- H: Set of industrial heating units.
- S: Set of storage units.
- N: Set of nodes in the network.
- B: Set of transmission branches.

Variables:

- ω_t: Weighting factor for operational and fuel cost in time period t.
- $o_{g,t}$: Variable operational & maintenance cost coefficient for generation unit g at time t.
- $o_{h,t}$: Variable operational & maintenance cost coefficient for industrial heating unit h at time t.
- $o_{s,t}$: Variable operational & maintenance cost coefficient for storage unit s at time t.
- $F_{g,t}$: Fuel cost coefficient for generation unit g at time t.
- $F_{h,t}$: Fuel cost coefficient for industrial heating unit h at time t.
- $p_{g,t}$: Power output of generation unit g at time t.
- $h_{g,t}$: Power output of industrial heating unit g at time t.
- C_g: Capital cost for generation unit g.
- C_h: Capital cost for industrial heating unit h.
- C_s: Capital cost for storage unit s.
- $\bar{p}_g$: Nominal capacity of power generation unit g.
- $\bar{h}_h$: Nominal capacity of industrial heating unit h.
- $\bar{S}_s$: Nominal capacity of storage unit s.
- $\bar{p}_{\text{new},g}$: New capacity of power generation unit g.
- $\bar{h}_{\text{new},g}$: New capacity of industrial heating unit g.
- $\bar{S}_{\text{new},s}$: New capacity of storage unit s.
- $\bar{p}^{\max}_g$: Maximum allowable capacity of power generation unit g.
- $\bar{h}^{\max}_g$: Maximum allowable capacity of industrial heating unit g.
- M_g: Fixed operational & maintenance cost for generation unit g.
- M_h: Fixed operational & maintenance cost for industrial heating unit h.
- M_s: Fixed operational & maintenance cost for storage unit s.
- $K_{b,n}$: Incidence matrix entry for branch b and node n.
- $DP_{t,n}$: Power demand for load at node n and time t.
- $DH_{t,n}$: Heating demand for load at node n and time t.
- $f^{\min}_{b,t}$: Minimum fraction of nominal flow capacity for branch b at time t.
- $f^{\max}_{b,t}$: Maximum fraction of nominal flow capacity for branch b at time t.
- $f_{b,t}$: Power flow of branch b at time t.
- e_d: Emission rate coefficient of component d.
- E: Maximum allowable emissions for the entire planning period.
- γ_d: Capacity credit for component d used in planning reserve margin (PRM) calculations.
- PRM: Planning reserve margin requirement.
- $SOC_{s,t}$: State of charge of storage unit s at time t.
- $S^{\text{in}}_{s,t}$: Charging power from storage unit s at time t.
- $S^{\text{out}}_{s,t}$: Discharge power from storage unit s at time t.
- η^{in}: Charging efficiency of storage.
- η^{out}: Discharging efficiency of storage.

Appendix B. Industrial process heating demand

See Table B.1.

Appendix C. Updates on subsurface temperature

We compared the subsurface temperature data used in this study [103,104] to earlier maps from Southern Methodist University (SMU; [105]), particularly at depths exceeding 4 kilometers (Fig. C.1).

At 4 km depth, western states like Idaho, California, and Oregon exhibit temperature increases of over 60 °C compared to previous studies, while eastern states also show approximately 20 °C higher values. On the other hand, Texas and other Gulf Coast states show cooler underground temperatures. It suggests that in most regions, geothermal resources can be accessed at shallower depths, reducing drilling costs compared to earlier estimates.

At depths of up to 7 km, states like Idaho could observe temperature increases exceeding 150 °C over previous estimates. The abundance of high-quality geothermal resources at greater depths emphasizes the potential for EGS plant development if drilling costs are reduced.

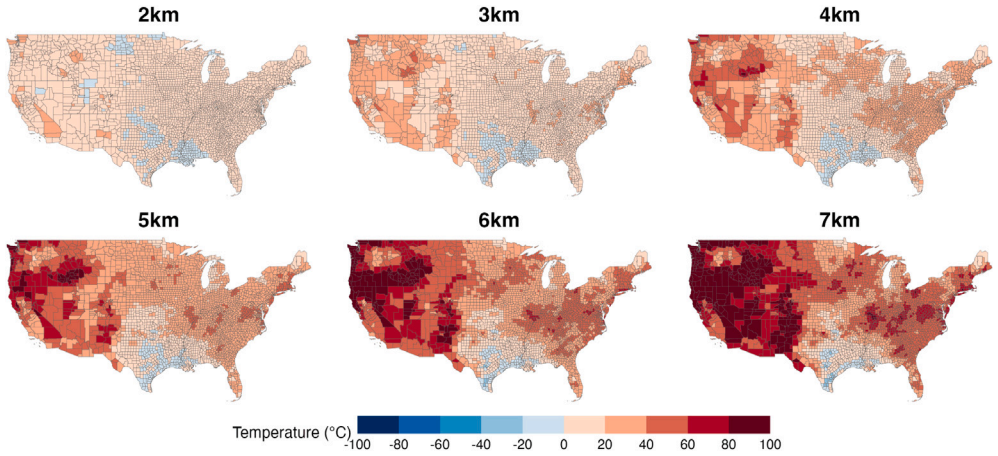

Fig. C.1. Temperature differences between [104] and SMU maps [105] from 2 to 7 km underground; regions shaded in red indicate areas where the temperature estimates from Aljubran and Horne [104] are higher than those from the SMU maps, and blue shows the opposite.

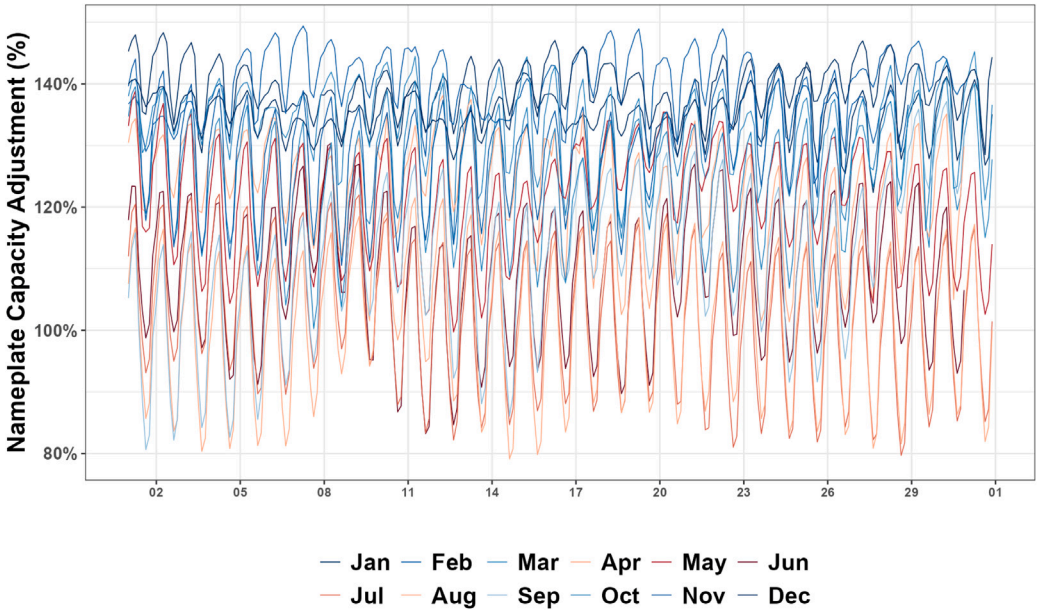

Fig. D.1. Nameplate capacity adjustment of EGS built in 2030 varied by months.

Appendix D. Influence of ambient temperature on capacity factor

Ambient temperature significantly affects the heat exchange efficiency of EGS, as noted in prior studies [10,114]. While air-cooled ORC power plants offer various benefits, their output varies with ambient temperature, wind speed, and humidity. In GEOPHIRES, we assumed an EGS binary plant ambient temperature of 10 °C, adjusting the nameplate capacity based on deviations from this design temperature using a relationship established in [10] with data from Turkey's Dora 1 ORC geothermal plant. Low ambient temperatures (< 0 °C) can increase the nameplate capacity up to 120%, while temperatures above 30 °C in summer can reduce output to 60% of nameplate capacity (Fig. D.1). The meteorology data above-mentioned provided average hourly temperatures for all regions, and this adjustment was applied to all potential EGS plants in the study.

Fig. D.2 presents the model estimation of power generation in the WECC region over an entire year. EGS contributes significantly during most seasons due to its high capacity factor and consistent output. However, during the summer months, EGS generation decreases substantially as gas plants ramp up to meet the additional power requirements. Outside of summer, the gas plants utilization would be low but play the role to meet the reserve margin. Fig. D.3 shows the capacity factors for all plant types in the WECC.

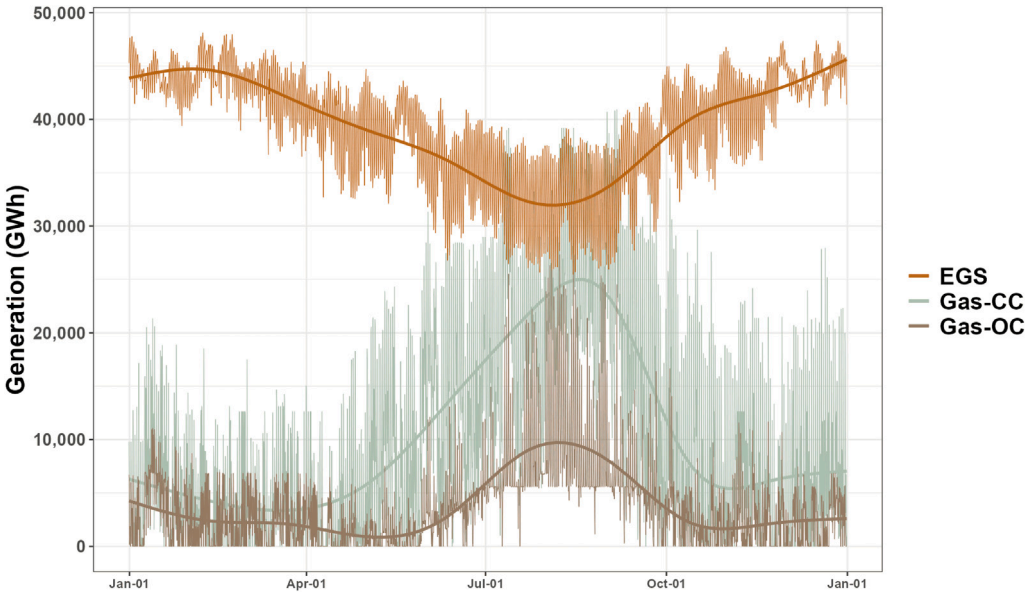

Fig. D.2. Hourly generation (GWh) of EGS compared to gas plants in the WECC in 2030.

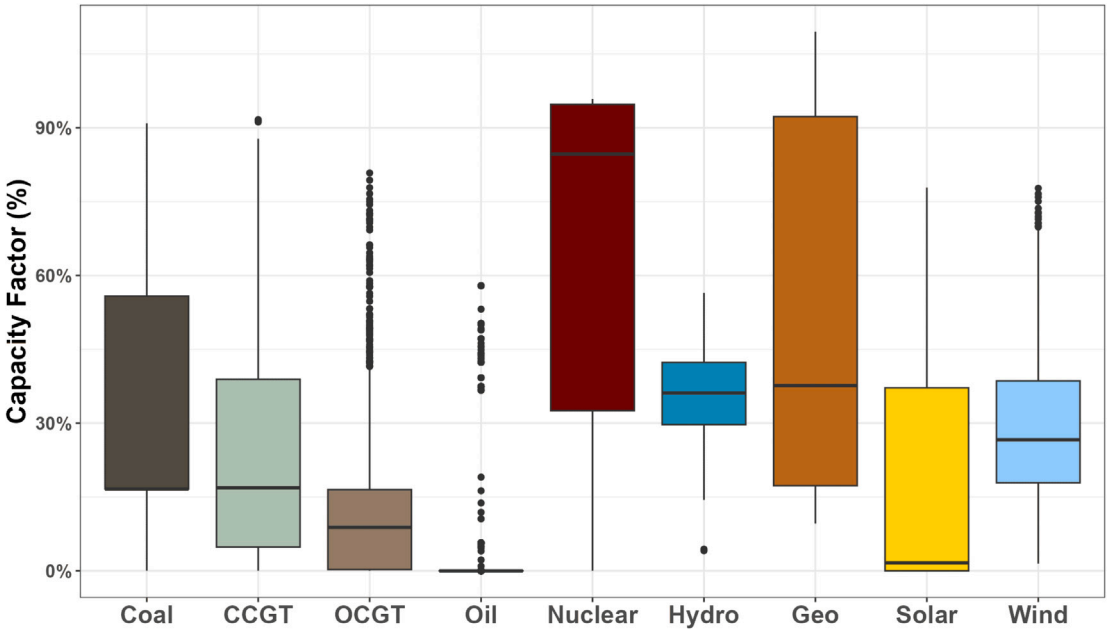

Fig. D.3. Boxplot shows capacity factors in the WECC of all plant types in 2030.

Appendix E. Sensitivity analysis: Fuel cost

Natural gas prices for industrial consumers in the United States have historically varied significantly across months and states due to regional supply–demand dynamics, infrastructure availability, and local market conditions (Fig. E.1). This study incorporates a sensitivity analysis to address the volatility of natural gas prices, which are influenced by weather fluctuations, technical disruptions, and geopolitical events. Figs. E.2 and E.3 illustrate how power generators and heating fleets in WECC and ERCOT respond to scenarios of high and low natural gas prices. Additionally, Figs. E.4 and E.5 compare heating fleet capacities under current 2023 EIA fuel costs and projected costs from the AEO for 2030.

Appendix F. Sensitivity analysis: IRA

To account for the potential repeal of the Inflation Reduction Act (IRA), we conducted an additional sensitivity analysis comparing scenarios with and without IRA incentives (Table F.1). In the IRA scenario (main case), eligible clean electricity projects can choose between the Production Tax Credit (PTC) and the Investment Tax Credit (ITC). We model the PTC as a $27.50/MWh credit for onshore wind, solar, and biomass, and the ITC as a 30% tax credit for offshore wind, geothermal, small modular reactors (SMRs), and all energy storage systems. In the No IRA scenario, these incentives are removed, resulting in higher capital costs for the affected technologies.

Without the IRA, wind deployment declines across all three interconnections, while solar remains relatively unaffected. The most significant impact is observed in geothermal EGS: nearly half of the

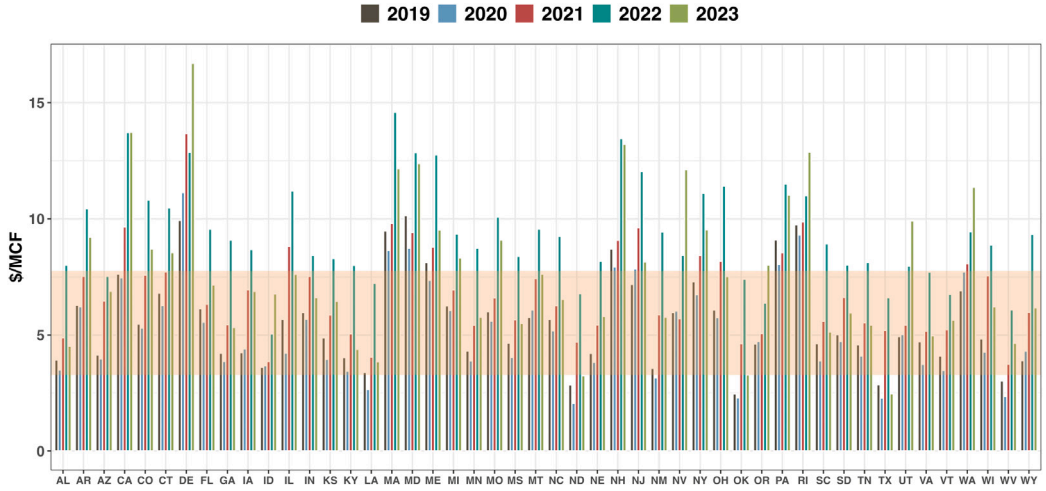

Fig. E.1. Annual natural gas price for industrial use ($/MCF) from 2019 to 2023 for all states. The orange band indicates the U.S. average in each year.

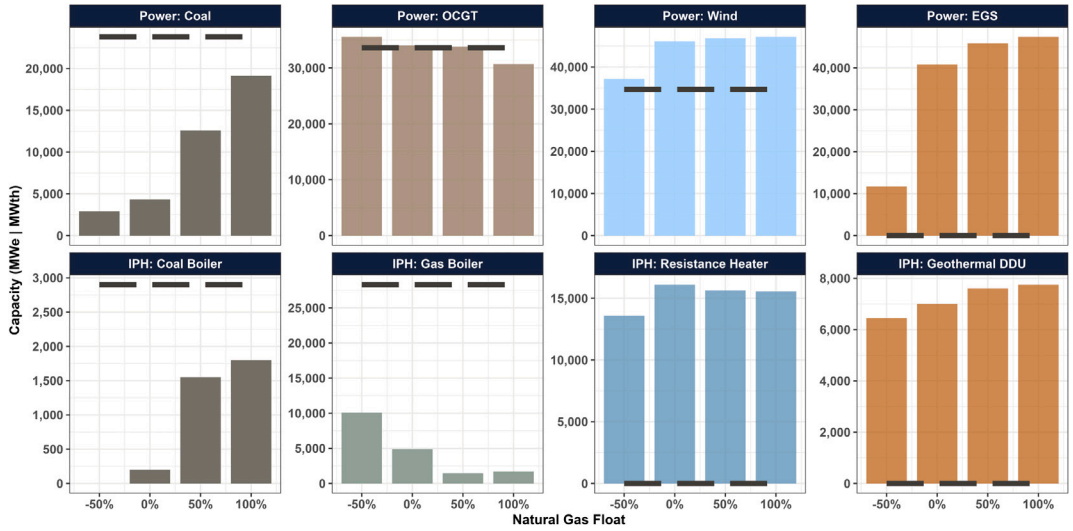

Fig. E.2. Sensitivity analysis of natural gas price volatility (−50%, 0%, 50%, 100%) in WECC and impacts on plant type; the dashed line indicates the 2023 baseline capacity.

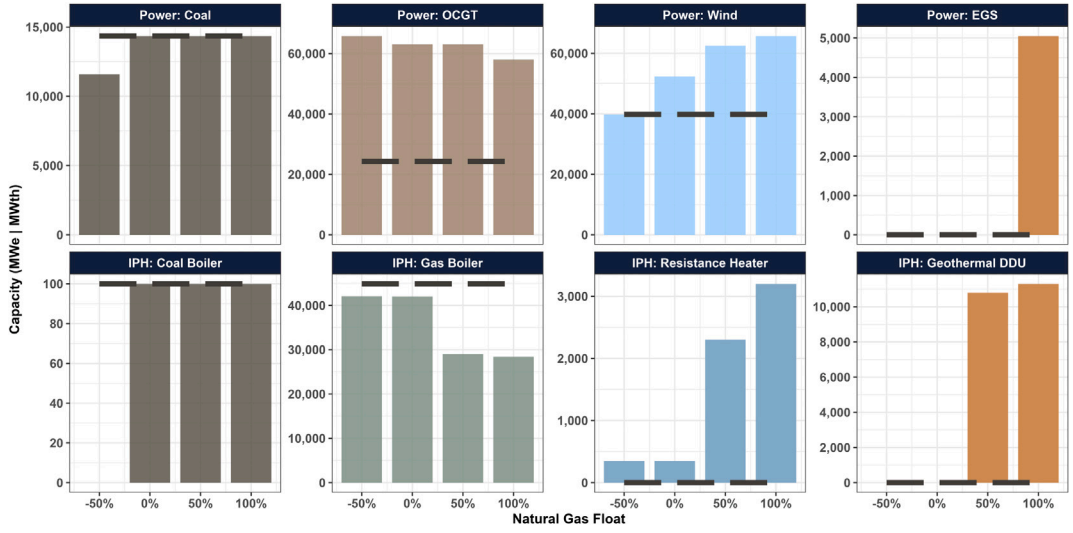

Fig. E.3. Sensitivity analysis of natural gas price volatility (−50%, 0%, 50%, 100%) in ERCOT and impacts on plant type; the dashed line indicates the 2023 baseline capacity.

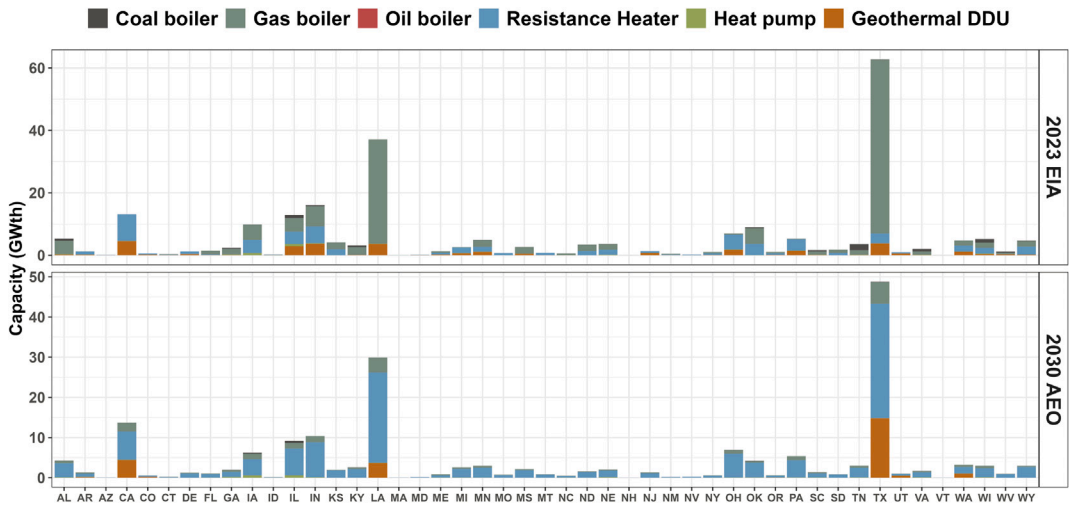

Fig. E.4. Heating appliances capacity by states (GW_{th}) comparing the 2023 EIA natural gas prices to the AEO predicted natural gas price in 2030.

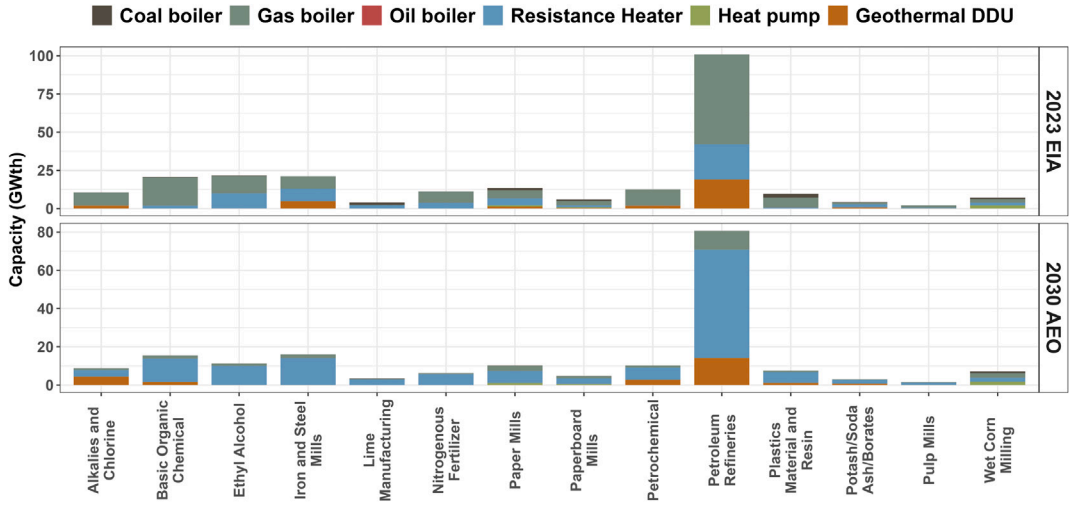

Fig. E.5. Heating appliances capacity by NAICS (GW_{th}) comparing the 2023 EIA natural gas prices to the AEO predicted natural gas price in 2030.

Table F.1
Capacity of heating (GW_{th}) and power generation (GW_e) plants under IRA and No IRA scenarios. The combined CO_2 emissions annually are summarized in the last row.

		Eastern		ERCOT		Western	
		IRA	No IRA	IRA	No IRA	IRA	No IRA
Heating (GW_{th})	Coal boiler	8.4	8.9	0.1	0.1	0.2	1.3
	Gas boiler	96.8	95.8	42.0	42.0	4.9	5.2
	Geothermal DDU	23.1	25.3	0.0	0.0	7.0	8.0
	Heat pump	3.2	2.9	0.0	0.0	0.1	0.0
	Resistance heater	43.2	30.7	0.3	0.3	16.1	14.9
Power (GW_e)	CCGT	275.8	293.3	42.1	42.1	45.2	59.6
	Coal	114.8	112.7	14.3	14.3	4.3	8.2
	EGS	0.1	0.1	0.0	0.0	40.0	22.7
	OCGT	280.2	265.0	63.1	63.1	34.0	34.0
	Solar	78.0	77.9	32.5	32.5	49.4	49.3
	Wind	175.4	83.0	52.4	39.8	46.1	34.7
Combined CO_2 (Mt)		501.3	561.5	31.7	103.2	27.9	62.4

previously projected capacity, or nearly 18 GW_e, would not be developed due to the lack of ITC which significantly raises capital costs. This shortfall is largely offset by increased reliance on fossil generation, with an additional 17.4 GW_e and 14.2 GW_e of CCGT capacity added in the Eastern and Western interconnections, respectively.

Higher electricity prices in the No IRA scenario also hinder industrial heating electrification. Nationally, 13.8 GW_{th} of resistance heating and 0.3 GW_{th} of heat pump capacity would no longer be deployed. However, this shift slightly benefits geothermal DDU, which increases by 3.2 GW_{th} as it becomes more competitive relative to

electric heating. Coal boiler use also rises, increasing by 17.4% without the IRA.

Overall, the repeal of the IRA would substantially hinder the deployment of wind and EGS, increase reliance on fossil fuel-based generation, elevate electricity prices, and reduce adoption of electric heating technologies such as resistance heaters and heat pumps. In term of CO_2 emissions, PyPSA simulates that repealing the IRA would lead to a significant increase in CO_2 emissions from both the power and IPH sectors. Annual emissions would rise by 60.2 Mt in the Eastern interconnection, 71.5 Mt in ERCOT, and 34.5 Mt in the Western interconnection, totaling an additional 166.2 Mt of CO_2 nationwide. This represents a 30% increase in total emissions compared to the IRA scenario, potentially delaying progress toward national decarbonization targets. Our modeling should not be taken as a simulation of the full effects of IRA repeal, since we do not consider aspects such as incentives for electric cars, hydrogen, carbon capture, or domestic manufacturing.

Data availability

Data will be made available on request.

References

[1] Sharmin Tasnuva, Khan Nazia Rodoshi, Akram Md Saleh, Ehsan M Monjurul. A State-of-the-Art Review on Geothermal Energy Extraction, Utilization, and Improvement Strategies: Conventional, Hybridized, and Enhanced Geothermal Systems. Int J Thermofluids 2023;18:100323. http://dx.doi.org/10.1016/j.ijft.2023.100323, URL https://www.sciencedirect.com/science/article/pii/S2666202723000423.

[2] Beckers Koenraad F, Kolker Amanda, Pauling Hannah, McTigue Joshua D, Kesseli Devon. Evaluating the feasibility of geothermal deep direct-use in the United States. Energy Convers Manage 2021;243:114335. http://dx.doi.org/10.1016/j.enconman.2021.114335, URL https://www.sciencedirect.com/science/article/pii/S0196890421005112.

[3] US DOE. Electricity generation. U.S. DOE; 2025, URL https://www.energy.gov/eere/geothermal/electricity-generation.

[4] Snyder Diana M, Beckers Koenraad F, Young Katherine R. Update on Geothermal Direct-use Installations in the United States. In: Proceedings, 42nd workshop on geothermal reservoir engineering. SGP-TR-212, 2017.

[5] Robins Jody, Kolker Amanda, Flores-Espino Francisco, Pettitt Will, Schmidt Brian, Beckers Koenraad, Pauling Hannah, Anderson Ben. 2021 U.S. geothermal power production and district heating market report. Technical report NREL/TP-5700-78291, 1808679, MainId:32208, 2021, URL https://www.osti.gov/servlets/purl/1808679/.

[6] IRENA. Global geothermal market and technology assessment. IRENA; 2023, URL https://www.irena.org/Publications/2023/Feb/Global-geothermal-market-and-technology-assessment.

[7] Livescu Silviu, Dindoruk Birol, Schulz Rebecca, Boul Peter, Kim Jihoon, Wu Kan. Chapter 1: Geothermal and electricity production: scalable geothermal concepts in the future of geothermal in texas: contemporary prospects and perspectives. Technical report, The University of Texas at Austin; 2023, URL https://repositories.lib.utexas.edu/bitstream/handle/2152/117202/Chapter1.pdf.

[8] Augustine Chad, Fisher Sarah, Ho Jonathan, Warren Ian, Witter Erik. Enhanced geothermal shot analysis for the geothermal technologies office. Technical report NREL/TP-5700-84822, National Renewable Energy Laboratory (NREL), Golden, CO (United States); 2023, URL https://www.osti.gov/biblio/1922621.

[9] Chen Chen, Merino-Garcia Daniel, Lines Timothy DGH, Cohan Daniel S. Geothermal power generation potential in the United States by 2050. Environ Res: Energy 2024;1(2):025003. http://dx.doi.org/10.1088/2753-3751/ad3fbb, Publisher: IOP Publishing.

[10] Ricks Wilson, Voller Katharine, Galban Gerame, Norbeck Jack H, Jenkins Jesse D. The role of flexible geothermal power in decarbonized electricity systems. Nat Energy 2024;1–13. http://dx.doi.org/10.1038/s41560-023-01437-y, URL https://www.nature.com/articles/s41560-023-01437-y. Publisher: Nature Publishing Group.

[11] US DOE. GeoVision: Harnessing the heat beneath our feet. Department of Energy; 2019, URL https://www.energy.gov/sites/default/files/2019/06/f63/GeoVision-full-report-opt.pdf.

[12] McTigue Joshua D, Wendt Daniel, Kitz Kevin, Gunderson Joshua, Kincaid Nick, Zhu Guangdong. Assessing geothermal/solar hybridization – Integrating a solar thermal topping cycle into a geothermal bottoming cycle with energy storage. Appl Therm Eng 2020;171:115121. http://dx.doi.org/10.1016/j.applthermaleng.2020.115121, URL https://www.sciencedirect.com/science/article/pii/S1359431119356960.

[13] Limberger Jon, Boxem Thijs, Pluymaekers Maarten, Bruhn David, Manzella Adele, Calcagno Philippe, Beekman Fred, Cloetingh Sierd, van Wees Jan-Diederik. Geothermal energy in deep aquifers: A global assessment of the resource base for direct heat utilization. Renew Sustain Energy Rev 2018;82:961–75. http://dx.doi.org/10.1016/j.rser.2017.09.084, URL https://www.sciencedirect.com/science/article/pii/S1364032117313345.

[14] Willems CJL, Nick HM, Goense T, Bruhn DF. The impact of reduction of doublet well spacing on the Net Present Value and the life time of fluvial Hot Sedimentary Aquifer doublets. Geothermics 2017;68:54–66. http://dx.doi.org/10.1016/j.geothermics.2017.02.008, URL https://www.sciencedirect.com/science/article/pii/S037565051630147X.

[15] Toews Matthew, Holmes Michael. Eavor-Lite Performance Update and Extrapolation to Commercial Projects. GRC Trans 2021;45.

[16] Yu Han, Xu Tianfu, Yuan Yilong, Gherardi Fabrizio, Tian Hailong. Single well geothermal heating systems: Technical and economic assessment of two widely-used configurations. J Hydrol 2024;635:131126. http://dx.doi.org/10.1016/j.jhydrol.2024.131126, URL https://www.sciencedirect.com/science/article/pii/S0022169424005213.

[17] Axelsson Gudni. Sustainable geothermal utilization – Case histories; definitions; research issues and modelling. Geothermics 2010;39(4):283–91. http://dx.doi.org/10.1016/j.geothermics.2010.08.001, URL https://www.sciencedirect.com/science/article/pii/S0375650510000404.

[18] Turchi Craig S, Akar Sertac, Cath Tzahi, Vanneste Johan, Geza Mengistu. Use of low-temperature geothermal energy for desalination in the western United States. Technical report NREL/TP–5500-65277, 1227955, 2015, URL http://www.osti.gov/servlets/purl/1227955/.

[19] Turchi Craig, McTigue Joshua Dominic, Akar Sertac, Beckers Koenraad, Richards Maria, Chickering Cathy, Batir Joseph, Schumann Harrison, Tillman Tom, Slivensky David. Geothermal deep direct use for turbine inlet cooling in east Texas. Technical report NREL/TP–5500-74990, 1602704, 2020, URL https://www.osti.gov/servlets/purl/1602704/.

[20] IEA. Net zero by 2050 - a roadmap for the global energy sector. IEA; 2021, URL https://iea.blob.core.windows.net/assets/deebef5d-0c34-4539-9d0c-10b13d840027/NetZeroby2050-ARoadmapfortheGlobalEnergySector_CORR.pdf.

[21] Peng Xu, Sun Laixiang, Feng Kuishuang, Zhong Honglin, Liang Jing, Zhang Chao, Zhao Dandan, Chen Hong, Long Ruyin, Xing Zhencheng, Hubacek Klaus. Extent of global decarbonization of the power sector through energy policies and governance capacity. Commun Earth & Environ 2024;5(1):1–9. http://dx.doi.org/10.1038/s43247-024-01494-5, URL https://www.nature.com/articles/s43247-024-01494-5. Publisher: Nature Publishing Group.

[22] Jacobson Mark Z, Krauland Anna-Katharina von, Coughlin Stephen J, Dukas Emily, Nelson Alexander JH, Palmer Frances C, Rasmussen Kylie R. Low-cost solutions to global warming, air pollution, and energy insecurity for 145 countries. Energy & Environ Sci 2022;15(8):3343–59. http://dx.doi.org/10.1039/D2EE00722C, URL https://pubs.rsc.org/en/content/articlelanding/2022/ee/d2ee00722c. Publisher: The Royal Society of Chemistry.

[23] Jafari Mehdi, Botterud Audun, Sakti Apurba. Decarbonizing power systems: A critical review of the role of energy storage. Renew Sustain Energy Rev 2022;158:112077. http://dx.doi.org/10.1016/j.rser.2022.112077, URL https://www.sciencedirect.com/science/article/pii/S1364032122000077.

[24] Browning Morgan, McFarland James, Bistline John, Boyd Gale, Muratori Matteo, Binsted Matthew, Harris Chioke, Mai Trieu, Blanford Geoff, Edmonds Jae, Fawcett Allen A, Kaplan Ozge, Weyant John. Net-zero CO2 by 2050 scenarios for the United States in the Energy Modeling Forum 37 study. Energy Clim Chang 2023;4:100104. http://dx.doi.org/10.1016/j.egycc.2023.100104, URL https://www.sciencedirect.com/science/article/pii/S2666278723000119.

[25] Bistline John E, Hodson Elke, Rossmann Charles G, Creason Jared, Murray Brian, Barron Alexander R. Electric sector policy, technological change, and U.S. emissions reductions goals: Results from the EMF 32 model intercomparison project. Energy Econ 2018;73:307–25. http://dx.doi.org/10.1016/j.eneco.2018.04.012, URL https://www.sciencedirect.com/science/article/pii/S0140988318301373.

[26] Jayadev Gopika, Leibowicz Benjamin D, Kutanoglu Erhan. U.S. electricity infrastructure of the future: Generation and transmission pathways through 2050. Appl Energy 2020;260:114267. http://dx.doi.org/10.1016/j.apenergy.2019.114267, URL https://www.sciencedirect.com/science/article/pii/S0306261919319543.

[27] Sepulveda Nestor A, Jenkins Jesse D, de Sisternes Fernando J, Lester Richard K. The Role of Firm Low-Carbon Electricity Resources in Deep Decarbonization of Power Generation. Joule 2018;2(11):2403–20. http://dx.doi.org/10.1016/j.joule.2018.08.006, URL https://www.sciencedirect.com/science/article/pii/S2542435118303866.

[28] Larson Eric, Greig Chris, Jenkins Jesse, Mayfield Erin, Pascale Andrew, Zhang Chuan, Drossman Joshua, Williams Robert, Pacala Steve, Socolow Robert, et al. Net-Zero America: Potential pathways, infrastructure, and impacts. Princet Univ 2021.

[29] US EIA. Annual Electric Power Industry Report, Form EIA-860 detailed data with previous form data (EIA-860A/860B). 2024, URL https://www.eia.gov/electricity/data/eia860/index.php.

[30] US DOE. Manufacturing Energy and Carbon Footprints. 2022.
[31] US DOE. Process heat basics. Department of Energy; 2024, URL https://www.energy.gov/eere/iedo/process-heat-basics.
[32] US DOE. Industrial heat shot. U.S. DOE; 2024, URL https://www.energy.gov/topics/industrial-heat-shot.
[33] Rissman Jeffrey. Decarbonizing low-temperature industrial heat in the U.S.. Energy Innovation Policy Technology LLC; 2022, URL https://energyinnovation.org/wp-content/uploads/2022/10/Decarbonizing-Low-Temperature-Industrial-Heat-In-The-U.S.-Report-2.pdf.
[34] Friedmann S Julio, Fan Zhiyuan, Tang Ke. Low-carbon heat solutions for heavy industry: sources, options, and costs today. 2019.
[35] McCabe Kevin, Gleason Michael, Reber Tim, Young Katherine R. Characterizing U.S. Heat Demand for Potential Application of Geothermal Direct Use: Preprint. 2016.
[36] B. Fox Don, Sutter Daniel, W. Tester Jefferson. The thermal spectrum of low-temperature energy use in the United States. Energy & Environ Sci 2011;4(10):3731–40. http://dx.doi.org/10.1039/C1EE01722E, URL https://pubs.rsc.org/en/content/articlelanding/2011/ee/c1ee01722e. Publisher: Royal Society of Chemistry.
[37] Kurup Parthiv, Turchi Craig. Initial investigation into the potential of CSP industrial process heat for the southwest United States. Technical report NREL/TP-6A20-64709, National Renewable Energy Lab. (NREL), Golden, CO (United States); 2015, URL https://www.osti.gov/biblio/1227710.
[38] McMillan Colin, Xi William, Zhang Jingyi, Masanet Eric, Kurup Parthiv, Schoeneberger Carrie, Meyers Steven, Margolis Robert. Evaluating the economic parity of solar for industrial process heat. Sol Energy Adv 2021;1:100011. http://dx.doi.org/10.1016/j.seja.2021.100011, URL https://linkinghub.elsevier.com/retrieve/pii/S2667113121000115.
[39] Xia Li, Liu Renmin, Zeng Yiting, Zhou Peng, Liu Jingjing, Cao Xiaorong, Xiang Shuguang. A review of low-temperature heat recovery technologies for industry processes. Chin J Chem Eng 2019;27(10):2227–37. http://dx.doi.org/10.1016/j.cjche.2018.11.012, URL https://www.sciencedirect.com/science/article/pii/S1004954118314356.
[40] McMillan Colin, Ruth Mark. Industrial process heat demand characterization. National Renewable Energy Laboratory - Data (NREL-DATA), Golden, CO (United States); National Renewable Energy Laboratory; 2018, http://dx.doi.org/10.7799/1461488, URL https://www.osti.gov/servlets/purl/1461488/. Artwork Size: 1 files Pages: 1 files.
[41] US EIA. Total energy monthly data. U.S. Energy Information Administration (EIA); 2024, URL https://www.eia.gov/totalenergy/data/monthly/index.php.
[42] El-Sadi Kareem, Gierke Brittany, Howard Elliot, Gradl Christian. Review of drilling performance in a horizontal EGS development. In: Proceedings, 49th stanford workshop on geothermal reservoir engineering. 2024.
[43] Meta. New Geothermal Energy Project to Support Our Data Centers. 2024, Meta, URL https://about.fb.com/news/2024/08/new-geothermal-energy-project-to-support-our-data-centers/.
[44] Rivas Mauricio, McGuire Victoria, Simpkins Douglas, Ring Lev. Geopressured Geothermal Systems: An Efficient and Sustainable Heat Extraction Method. 2024.
[45] Stumpf Andrew, Damico James, Okwen Roland, Stark Timothy, Elrick Scott, John W, Lu Yongqi, Holcomb Franklin, Tinjum James, Yang Fang, Frailey Scott, Lin Yu-Feng. Feasibility of a Deep Direct-Use Geothermal System at the University of Illinois Urbana-Champaign. 2018.
[46] Lowry Thomas Stephen, Ayling Bridget, Hinz Nicholas, Sabin Andrew, Arguello Raymond, Blake Kelly, Tiedeman Andy. Deep direct-use geothermal feasibility study for hawthorne NV. Technical report SAND-2020-3210, Sandia National Lab. (SNL-NM), Albuquerque, NM (United States); 2020, URL https://www.osti.gov/biblio/1606296.
[47] Tester Jefferson, Jordan Teresa, Beyers Steve, Gustafson Olaf, Smith Jared. Earth source heat: a cascaded systems approach to DDU of geothermal energy on the cornell campus. Technical report DOE-Cornell-8103-1, Cornell Univ., Ithaca, NY (United States); 2019, URL https://www.osti.gov/biblio/1844600.
[48] Garapati Nagasree. Feasibility of deep direct-use geothermal on the west Virginia University Campus-Morgantown, WV. Technical report Final Technical Report-DOE-WVU, West Virginia Univ., Morgantown, WV (United States); 2021, URL https://www.osti.gov/biblio/1829981.
[49] Oh Hyunjun, Akar Sertaç, Beckers Koenraad, Bonnema Eric, Vivas Cesar, Salehi Saeed. Techno-economic feasibility of geothermal energy production using inactive oil and gas wells for district heating and cooling systems in Tuttle, Oklahoma. Energy Convers Manage 2024;308:118390. http://dx.doi.org/10.1016/j.enconman.2024.118390, URL https://www.sciencedirect.com/science/article/pii/S0196890424003315.
[50] Thiel Gregory P, Stark Addison K. To decarbonize industry, we must decarbonize heat. Joule 2021;5(3):531–50. http://dx.doi.org/10.1016/j.joule.2020.12.007, URL https://www.cell.com/joule/abstract/S2542-4351(20)30575-4. Publisher: Elsevier.
[51] Rissman Jeffrey, Bataille Chris, Masanet Eric, Aden Nate, Morrow William R, Zhou Nan, Elliott Neal, Dell Rebecca, Heeren Niko, Huckestein Brigitta, Cresko Joe, Miller Sabbie A, Roy Joyashree, Fennell Paul, Cremmins Betty, Koch Blank Thomas, Hone David, Williams Ellen D, de la Rue du Can Stephane, Sisson Bill, Williams Mike, Katzenberger John, Burtraw Dallas, Sethi Girish, Ping He, Danielson David, Lu Hongyou, Lorber Tom, Dinkel Jens, Helseth Jonas. Technologies and policies to decarbonize global industry: Review and assessment of mitigation drivers through 2070. Appl Energy 2020;266:114848. http://dx.doi.org/10.1016/j.apenergy.2020.114848, URL https://www.sciencedirect.com/science/article/pii/S0306261920303603.
[52] Bernath Christiane, Deac Gerda, Sensfuß Frank. Impact of sector coupling on the market value of renewable energies – a model-based scenario analysis. Appl Energy 2021;281:115985. http://dx.doi.org/10.1016/j.apenergy.2020.115985, URL https://www.sciencedirect.com/science/article/pii/S0306261920314331.
[53] Kirkerud Jon Gustav, Bolkesjø Torjus Folsland, Trømborg Erik. Power-to-heat as a flexibility measure for integration of renewable energy. Energy 2017;128:776–84. http://dx.doi.org/10.1016/j.energy.2017.03.153, URL https://www.sciencedirect.com/science/article/pii/S0360544217305479.
[54] Gea-Bermúdez Juan, Jensen Ida Græsted, Münster Marie, Koivisto Matti, Kirkerud Jon Gustav, Chen Yi-kuang, Ravn Hans. The role of sector coupling in the green transition: A least-cost energy system development in Northern-central Europe towards 2050. Appl Energy 2021;289:116685. http://dx.doi.org/10.1016/j.apenergy.2021.116685, URL https://www.sciencedirect.com/science/article/pii/S0306261921002130.
[55] Thellufsen Jakob Zinck, Lund Henrik. Cross-border versus cross-sector interconnectivity in renewable energy systems. Energy 2017;124:492–501. http://dx.doi.org/10.1016/j.energy.2017.02.112, URL https://www.sciencedirect.com/science/article/pii/S0360544217302943.
[56] Brown Tom, Schäfer Mirko, Greiner Martin. Sectoral Interactions as Carbon Dioxide Emissions Approach Zero in a Highly-Renewable European Energy System. Energies 2019;12(6):1032. http://dx.doi.org/10.3390/en12061032, URL https://www.mdpi.com/1996-1073/12/6/1032. Number: 6 Publisher: Multidisciplinary Digital Publishing Institute.
[57] Brown T, Schlachtberger D, Kies A, Schramm S, Greiner M. Synergies of sector coupling and transmission reinforcement in a cost-optimised, highly renewable European energy system. Energy 2018;160:720–39. http://dx.doi.org/10.1016/j.energy.2018.06.222, URL https://www.sciencedirect.com/science/article/pii/S036054421831288X.
[58] Victoria Marta, Zhu Kun, Brown Tom, Andresen Gorm B, Greiner Martin. The role of storage technologies throughout the decarbonisation of the sector-coupled European energy system. Energy Convers Manage 2019;201:111977. http://dx.doi.org/10.1016/j.enconman.2019.111977, URL https://www.sciencedirect.com/science/article/pii/S0196890419309835.
[59] Pavičević Matija, Mangipinto Andrea, Nijs Wouter, Lombardi Francesco, Kavvadias Konstantinos, Jiménez Navarro Juan Pablo, Colombo Emanuela, Quoilin Sylvain. The potential of sector coupling in future European energy systems: Soft linking between the Dispa-SET and JRC-EU-TIMES models. Appl Energy 2020;267:115100. http://dx.doi.org/10.1016/j.apenergy.2020.115100, URL https://www.sciencedirect.com/science/article/pii/S0306261920306127.
[60] Fridgen Gilbert, Keller Robert, Körner Marc-Fabian, Schöpf Michael. A holistic view on sector coupling. Energy Policy 2020;147:111913. http://dx.doi.org/10.1016/j.enpol.2020.111913, URL https://www.sciencedirect.com/science/article/pii/S0301421520306248.
[61] Ramsebner Jasmine, Haas Reinhard, Ajanovic Amela, Wietschel Martin. The sector coupling concept: A critical review. WIREs Energy Environ 2021;10(4):e396. http://dx.doi.org/10.1002/wene.396, URL https://onlinelibrary.wiley.com/doi/abs/10.1002/wene.396. _eprint: https://onlinelibrary.wiley.com/doi/pdf/10.1002/wene.396.
[62] Cochran Jaquelin, Denholm Paul, Mooney Meghan, Steinberg Daniel, Hale Elaine, Heath Garvin, Palmintier Bryan, Sigrin Ben, Keyser David, McCamey Devonie, Cowiestoll Brady, Horsey Kelsey, Fontanini Anthony, Jain Himanshu, Muratori Matteo, Jorgenson Jennie, Irish Matt, Ban-Weiss George, Cutler Harvey, Ravi Vikram, Nicholson Scott. LA100: The Los Angeles 100% Renewable Energy Study Executive Summary. 2021.
[63] Williams James H, Jones Ryan A, Haley Ben, Kwok Gabe, Hargreaves Jeremy, Farbes Jamil, Torn Margaret S. Carbon-Neutral Pathways for the United States. AGU Adv 2021;2(1). http://dx.doi.org/10.1029/2020AV000284, e2020AV000284. URL https://onlinelibrary.wiley.com/doi/abs/10.1029/2020AV000284. _eprint: https://onlinelibrary.wiley.com/doi/pdf/10.1029/2020AV000284.
[64] O'Connor Michael. Enhanced geothermal shot frequently asked questions. DOE; 2023, URL https://www.energy.gov/sites/default/files/2023-01/enhanced-geothermal-shot-faq_012023.pdf.
[65] Rangel Jurado Nicolas, Küçük Serhat, Brehme Maren, Lathion Rodolphe, Games Federico, Saar Martin. Comparative Analysis on the Techno-Economic Performance of Different Types of Deep Geothermal Systems for Heat Production. 2022.
[66] Olasolo P, Juárez MC, Olasolo J, Morales MP, Valdani D. Economic analysis of Enhanced Geothermal Systems (EGS). a review of software packages for estimating and simulating costs. Appl Therm Eng 2016;104:647–58. http://dx.doi.org/10.1016/j.applthermaleng.2016.05.073, URL https://www.sciencedirect.com/science/article/pii/S135943111630730X.

[67] Beckers Koenraad, Vasyliv Yaroslav, Bran-Anleu Gabriela A, Martinez Mario, Augustine Chad, White Mark. Tabulated Database of Closed-Loop Geothermal Systems Performance for Cloud-Based Technical and Economic Modeling of Heat Production and Electricity Generation: Preprint. Renew Energy 2023.
[68] Norbeck Jack Hunter, Gradl Christian, Latimer Timothy. Deployment of Enhanced Geothermal System technology leads to rapid cost reductions and performance improvements. 2024, URL https://eartharxiv.org/repository/view/7665/. Publisher: EarthArXiv.
[69] Baral Suresh, Šebo Juraj. Techno-economic assessment of green hydrogen production integrated with hybrid and organic Rankine cycle (ORC) systems. Heliyon 2024;10(4). http://dx.doi.org/10.1016/j.heliyon.2024.e25742, URL https://www.cell.com/heliyon/abstract/S2405-8440(24)01773-0. Publisher: Elsevier.
[70] Mines Gregory. GETEM user manual. Idaho National Laboratory; 2016, URL.
[71] Romanov Dmitry, Leiss Bernd. Analysis of Enhanced Geothermal System Development Scenarios for District Heating and Cooling of the Göttingen University Campus. Geosciences 2021;11(8):349. http://dx.doi.org/10.3390/geosciences11080349, URL https://www.mdpi.com/2076-3263/11/8/349. Number: 8 Publisher: Multidisciplinary Digital Publishing Institute.
[72] Tehranchi Kamran, Barnes Trevor, Frysztacki Martha, Azevedo Ines. Pypsa-Usa: A flexible open-source energy system model and optimization tool for the United States. Rochester, NY: Social Science Research Network; 2024, http://dx.doi.org/10.2139/ssrn.5029120, URL https://papers.ssrn.com/abstract=5029120.
[73] Hörsch Jonas, Hofmann Fabian, Schlachtberger David, Brown Tom. PyPSA-Eur: An open optimisation model of the European transmission system. Energy Strat Rev 2018;22:207–15. http://dx.doi.org/10.1016/j.esr.2018.08.012, URL https://www.sciencedirect.com/science/article/pii/S2211467X18300804.
[74] Hofmann Fabian, Hampp Johannes, Neumann Fabian, Brown Tom, Hörsch Jonas. Atlite: A Lightweight Python Package for Calculating Renewable Power Potentials and Time Series. J Open Source Softw 2021;6(62):3294. http://dx.doi.org/10.21105/joss.03294, URL https://joss.theoj.org/papers/10.21105/joss.03294.
[75] Staffell Iain, Brett Dan, Brandon Nigel, Hawkes Adam. A review of domestic heat pumps. Energy & Environ Sci 2012;5(11):9291–306. http://dx.doi.org/10.1039/C2EE22653G, URL https://pubs.rsc.org/en/content/articlelanding/2012/ee/c2ee22653g. Publisher: The Royal Society of Chemistry.
[76] Xu Yixing, Myhrvold Nathan, Sivam Dhileep, Mueller Kaspar, Olsen Daniel J, Xia Bainan, Livengood Daniel, Hunt Victoria, d'Orfeuil Benjamin Rouille, Muldrew Daniel, Ondreicka Merrielle, Bettilyon Megan. U.S. Test System with High Spatial and Temporal Resolution for Renewable Integration Studies. In: 2020 IEEE power & energy society general meeting. Montreal, QC, Canada: IEEE; 2020, p. 1–5. http://dx.doi.org/10.1109/PESGM41954.2020.9281850, URL https://ieeexplore.ieee.org/document/9281850/.
[77] Ho Jonathan, Becker Jonathon, Brown Maxwell, Brown Patrick, Chernyakhovskiy Ilya, Cohen Stuart, Cole Wesley, Corcoran Sean, Eurek Kelly, Frazier Will, Gagnon Pieter, Gates Nathaniel, Greer Daniel, Jadun Paige, Khanal Saroj, Machen Scott, Macmillan Madeline, Mai Trieu, Mowers Matthew, Murphy Caitlin, Rose Amy, Schleifer Anna, Sergi Brian, Steinberg Daniel, Sun Yinong, Zhou Ella. Regional Energy Deployment System (ReEDS) Model Documentation: Version 2020. Renew Energy 2021.
[78] Brown Patrick R, Barrows Clayton P, Wright Jarrad G, Brinkman Gregory L, Dalvi Sourabh, Zhang Jiazi, Mai Trieu. A general method for estimating zonal transmission interface limits from nodal network data. 2023, http://dx.doi.org/10.48550/arXiv.2308.03612, arXiv URL http://arxiv.org/abs/2308.03612. arXiv:2308.03612. [eess].
[79] Sergi Brian, Brown Patrick, Cole Wesley. Transmission Interface Limits for High-Spatial Resolution Capacity Expansion Modeling. 2024, URL https://research-hub.nrel.gov/en/publications/transmission-interface-limits-for-high-spatial-resolution-capacit.
[80] Mai Trieu T, Jadun Paige, Logan Jeffrey S, McMillan Colin A, Muratori Matteo, Steinberg Daniel C, Vimmerstedt Laura J, Haley Benjamin, Jones Ryan, Nelson Brent. Electrification futures study: scenarios of electric technology adoption and power consumption for the United States. Technical report NREL/TP–6A20-71500, 1459351, 2018, URL http://www.osti.gov/servlets/purl/1459351/.
[81] US EIA. Preliminary Monthly Electric Generator Inventory (based on Form EIA-860M as a supplement to Form EIA-860). 2024, URL https://www.eia.gov/electricity/data/eia860m/index.php.
[82] NREL. 2024 Electricity ATB Technologies and Data Overview. 2024, URL https://atb.nrel.gov/electricity/2024/index.
[83] NERC. 2023 Long-Term Reliability Assessment. 2023, URL https://www.nerc.com/pa/RAPA/ra/Reliability%20Assessments%20DL/NERC_LTRA_2023.pdf.
[84] McMillan Colin A, Ruth Mark. Using facility-level emissions data to estimate the technical potential of alternative thermal sources to meet industrial heat demand. Appl Energy 2019;239:1077–90. http://dx.doi.org/10.1016/j.apenergy.2019.01.077, URL https://www.sciencedirect.com/science/article/pii/S0306261919300807.
[85] EPRI. Load shape library version 8.0. EPRI; 2020, URL https://loadshape.epri.com/enduse.
[86] US DOE. Pathways to Commercial Liftoff: Industrial Decarbonization. 2023.
[87] IRENA. Technology cost and performance. 2016, URL https://www.irena.org/-/media/Irena/Files/REmap/IRENA_REmap_2030_technology_cost.xlsx.
[88] Danish Energy Agency. Technology data for generation of electricity and district heating. Danish Energy Agency and Energinet.dk; 2018, URL https://ens.dk/en/our-services/technology-catalogues/technology-data-generation-electricity-and-district-heating.
[89] US EIA, . EIA; 2024, URL https://www.eia.gov/dnav/ng/ng_pri_sum_a_EPG0_PIN_DMcf_a.htm.
[90] Schoeneberger Carrie, Zhang Jingyi, McMillan Colin, Dunn Jennifer B, Masanet Eric. Electrification potential of U.S. industrial boilers and assessment of the GHG emissions impact. Adv Appl Energy 2022;5:100089. http://dx.doi.org/10.1016/j.adapen.2022.100089, URL https://www.sciencedirect.com/science/article/pii/S2666792422000075.
[91] US EIA. Carbon dioxide emissions coefficients. U.S. EIA; 2024, URL https://www.eia.gov/environment/emissions/co2_vol_mass.php.
[92] Leak Jarrod. Decarbonisation with industrial heat pumps: Policy & program update from Australia. Australian Alliance for Energy Productivity; 2022, URL https://www.aceee.org/sites/default/files/pdfs/Presentations/2022_International_Symposium/Jarrod_Leak.pdf.
[93] Jibran S. Zuberi M, Hasanbeigi Ali, Morrow William. Bottom-up assessment of industrial heat pump applications in U.S. Food manufacturing. Energy Convers Manage 2022;272:116349. http://dx.doi.org/10.1016/j.enconman.2022.116349, URL https://linkinghub.elsevier.com/retrieve/pii/S019689042201127X.
[94] IGA. Geothermal energy database. International Geothermal Association; 2023, URL https://worldgeothermal.org/geothermal-data/geothermal-energy-database.
[95] Akar Sertac, Kurup Parthiv, McTigue Joshua, Cox Jordan, Belding Scott, McMillan Colin, Lowder Travis, Baldwin Samuel. Renewable Thermal Energy Systems Designed for Industrial Process Solutions in Multiple Industries. In: Proceedings of the ISES solar world congress 2021. Virtual: International Solar Energy Society; 2021, p. 1–12. http://dx.doi.org/10.18086/swc.2021.29.01, URL http://proceedings.ises.org/citation?doi=swc.2021.29.01.
[96] US EIA. Form EIA-923 detailed data with previous form data (EIA-906/920). U.S. Energy Information Administration (EIA); 2024, URL https://www.eia.gov/electricity/data/eia923/index.php.
[97] Suri Dhruv, Chalendar Jacques de, Azevedo Ines. What are the real implications for CO_2 as generation from renewables increases? 2024, http://dx.doi.org/10.48550/arXiv.2408.05209, arXiv URL http://arxiv.org/abs/2408.05209. arXiv:2408.05209.
[98] US EIA. Annual coal report 2022. EIA; 2023, URL https://www.eia.gov/coal/annual/pdf/acr.pdf.
[99] CARB. Executive Order B-30-15. 2015, URL https://archive.gov.ca.gov/archive/gov39/2015/04/29/news18938/index.html.
[100] Oregon Climate Action Commission. Oregon Climate Action Roadmap to 2030. 2023, URL https://static1.squarespace.com/static/59c554e0f09ca40655ea6eb0/t/64275befc3f5d82a60b981b2/1680301043241/2023-Climate-Action-Roadmap.pdf.
[101] RGGI. The Regional Greenhouse Gas Initiative. 2023, URL https://www.rggi.org/program-overview-and-design/program-review.
[102] US IRS. Section 45V credit for production of clean hydrogen; section 48(a)(15) election to treat clean hydrogen production facilities as energy property. Internal Revenue Service (IRS); 2023, URL https://www.federalregister.gov/documents/2023/12/26/2023-28359/section-45v-credit-for-production-of-clean-hydrogen-section-48a15-election-to-treat-clean-hydrogen.
[103] Aljubran Mohammad J, Horne Roland N. Power supply characterization of baseload and flexible enhanced geothermal systems. Sci Rep 2024;14(1):17619. http://dx.doi.org/10.1038/s41598-024-68580-8, URL https://www.nature.com/articles/s41598-024-68580-8. Publisher: Nature Publishing Group.
[104] Aljubran Mohammad J, Horne Roland N. Thermal Earth Model for the Conterminous United States Using an Interpolative Physics-Informed Graph Neural Network (InterPIGNN). 2024, arXiv, URL http://arxiv.org/abs/2403.09961. arXiv:2403.09961.
[105] Blackwell David, Richards Maria, Frone Zachary, Batir Joe, Ruzo Andrés, Dingwall Ryan, Williams Mitchell. Temperature-at-depth maps for the conterminous US and geothermal resource estimates. Technical report GRC1029452, Southern Methodist University Geothermal Laboratory, Dallas, TX (United States); 2011, URL https://www.osti.gov/biblio/1137036.
[106] Ma Yongsheng. Deep geothermal resources in China: Potential, distribution, exploitation, and utilization. Energy Geosci 2023;4(4):100209. http://dx.doi.org/10.1016/j.engeos.2023.100209, URL https://www.sciencedirect.com/science/article/pii/S2666759223000550.
[107] Beckers Koenraad F, McCabe Kevin. GEOPHIRES v2.0: updated geothermal techno-economic simulation tool. Geotherm Energy 2019;7(1):5. http://dx.doi.org/10.1186/s40517-019-0119-6.
[108] Wu Bisheng, Zhang Xi, Jeffrey Robert G, Bunger Andrew P, Huddlestone-Holmes Cameron. Perturbation analysis for predicting the temperatures of water flowing through multiple parallel fractures in a rock mass. Int J Rock Mech Min Sci 2015;76:162–73. http://dx.doi.org/10.1016/j.ijrmms.2015.03.013, URL https://www.sciencedirect.com/science/article/pii/S1365160915000635.

[109] Ramey Jr HJ. Wellbore Heat Transmission. J Pet Technol 1962;14(04):427–35. http://dx.doi.org/10.2118/96-PA.
[110] Norbeck Jack Hunter, Latimer Timothy. Commercial-Scale Demonstration of a First-of-a-Kind Enhanced Geothermal System. 2023, URL https://eartharxiv.org/repository/view/5704/. Publisher: EarthArXiv.
[111] Lowry Thomas Stephen, Finger John T, Carrigan Charles R, Foris Adam, Kennedy Mack B, Corbet Thomas F, Doughty Christine A, Pye Steven, Sonnenthal Eric L. GeoVision analysis: reservoir maintenance and development task force report (geovision analysis supporting task force report : reservoir maintenance and development). Technical report SAND2017-9977, Sandia National Lab. (SNL-NM), Albuquerque, NM (United States); 2017, URL https://www.osti.gov/biblio/1394062.
[112] Fervo. Fervo Energy's Record-Breaking Production Results Showcase Rapid Scale Up Of Enhanced Geothermal - Fervo Energy. 2024, URL https://fervoenergy.com/fervo-energys-record-breaking-production-results-showcase-rapid-scale-up-of-enhanced-geothermal/. Section: Press Releases.
[113] Tester Jeff, Gustafson Olaf, Beyers Steve, Jordan Terry, Fulton Patrick. Geothermal Direct Use for Decarbonization - Progress Towards Demonstrating Earth Source Heat at Cornell. 2023.
[114] Karadas Murat, Celik H Murat, Serpen Umran, Toksoy Macit. Multiple regression analysis of performance parameters of a binary cycle geothermal power plant. Geothermics 2015;54:68–75. http://dx.doi.org/10.1016/j.geothermics.2014.11.003, URL https://www.sciencedirect.com/science/article/pii/S0375650514001333.
[115] US EPA. Greenhouse Gas Inventory Data Explorer. 2023, URL https://cfpub.epa.gov/ghgdata/inventoryexplorer/.
[116] IEA. The future of geothermal energy. IEA; 2024.
[117] McKinsey & Company. The future of next-generation geothermal energy | McKinsey. McKinsey & Company; 2025, URL https://www.mckinsey.com/industries/electric-power-and-natural-gas/our-insights/is-geothermal-energy-ready-to-make-its-mark-in-the-us-power-mix.
[118] Higgins Brian, Amaya Alvaro, Muir John, Scherer Joe. GreenFire energy closed-loop geothermal demonstration using supercritical carbon dioxide as working fluid. In: 45th workshop on geothermal reservoir engineering. 2020.
[119] Wang Gaosheng, Song Xianzhi, Shi Yu, Sun Baojiang, Zheng Rui, Li Jiacheng, Pei Zhijun, Song Hengyu. Numerical investigation on heat extraction performance of an open loop geothermal system in a single well. Geothermics 2019;80:170–84. http://dx.doi.org/10.1016/j.geothermics.2019.03.005, URL https://www.sciencedirect.com/science/article/pii/S0375650518302074.
[120] Tester Jeff, Beyers Steve, Gustafson J Olaf, Jordan Teresa E, Fulton Patrick M, Hawkins Adam J, Smith Jared D, Aswad Jood Al, Beckers Koenraad F, Allmendinger Rick, Brown Larry, Horowitz Frank, May Daniel, Ming Tasnuva, Pritchard Matt, Hall Snee. District Geothermal Heating Using EGS Technology to Meet Carbon Neutrality Goals: A Case Study of Earth Source Heat for the Cornell University Campus. 2021.